CHAPTER ONE
INTRODUCTION

1.1 General

Medical robots may be classified in many ways: by manipulator design (e.g., kinematics, actuation); by level of autonomy (e.g., preprogrammed versus teleoperation versus constrained cooperative control), by targeted anatomy or technique (e.g., cardiac, intravascular, percutaneous, laparoscopic, microsurgical) and by the intended operating environment [e.g., in-scanner, conventional operating room (OR)], etc,[1].

Traditional surgery requires an incision large enough for the surgeon to see directly and place his or her fingers and instruments directly into the target operating site. Most often, the damage done to skin, muscle, connective tissue, and bone to reach the region of interest causes much greater injury than the curative procedure itself. This results in more pain to the patient, longer recovery times, and complications due to surgical trauma. The accelerating trend is toward minimally invasive surgery (MIS), in which unnecessary trauma is limited by reducing the size of incisions to less than about 1 cm or by using catheters or endoscopes threaded through vessels, the gastrointestinal tract, [2].

1.2 The Fundamental Requirements From a Medical Robot

In order to insure the success of a medical robot, four fundamental requirements must be fulfilled. The first and most crucial requirement is safety. The following seven criteria constitute the safety requirements,[3].

1. Effective control: The robot must allow, in all configurations, effective control of the tool with both speed and force control schemes implemented.

2. Limited Workspace: The robot must have limited workspace in order to prevent hazardous collisions between its moving parts and the medical staff or the patient.
3. Limited Forces or Force feedback: In applications where the robot is active in performing surgical procedures that include tactile tasks, the force applied by the tool must be limited. Alternatively, in applications where the robot acts as a slave, the robot must convey a maximum amount of data to the surgeon about the forces exerted on the tool. This requirement is essential in the process of bone cutting where different levels of force are required during different stages of the cut.
4. Immunity against magnetic interference of other surgical tools.
5. Full control option: In applications where the robot performs automated tasks, the control program must allow the surgeon, in any stage in the task, to interrupt the automatic execution process and take over the control to his hands.
6. Fail safe features: The most reliable systems will inevitably fail in some stage of their service. Based on this premise the robot must support a fail-safe mode. This includes keeping the position of the tool when the power supply is lost, electrical limiting of the end effector's speed and force even when the control program fails.
7. Safe behavior near singular configurations: The path planning of the robot should avoid passing near singular configurations. However, in the cases where the robot acts as a slave, the surgeon might manipulate it into singular configurations.

` The second requirement from a medical robot is compactness in size and lightness. This ensures that the robot does not consume a large

amount of essential space in the operating room and facilitates the relocation of the robot in different positions for different tasks.

The third requirement is simple operation in order to improve the learning curve of new surgeons. The last, but not least important, requirement is the requirement for easy sterilization. This requirement is critical since any tool in the operating room must either be sterilized or covered with sterile drapes in order to prevent infections.

1.3 Medical Robotics, Classification of Surgical System

A general classification has been established for guiding systems in the surgical systems field, based on the type of interaction (also called degree of passivity) between the human operator and the device [4]:

(i)- Passive systems: In this type the surgeon is totally responsible for the execution of the surgical action. That means providing information to the surgeon. It has tracking characteristics of the object of interest and stability of positioning if the arm is equipped with brakes. But the drawbacks of passive systems are tracking of only one object, cumbersome, constraints the surgeon motion and limited to navigation.

(ii)- Active systems: They realize part of the intervention autonomously and the operator supervises the task. They perform the procedure under human supervision and use in tasks with a complex geometry, carry/hold heavy tools, force controlled actions and moving targets but expensive,[5]. Generally the surgical system has many advantages:

- optimal planning
- consistent and accurate execution
- safety
- validation

- information management

1.4 Surgical Robot Design Considerations

The mechanical design of a surgical robot depends crucially on its intended application. For example, robots with high precision, stiffness and (possibly) limited dexterity are often very suitable for orthopaedic bone shaping or stereotactic needle placement. Medical robots for these applications frequently have high gear ratios and consequently, low back-drivability, high stiffness, and low speed. On the other hand, robots for complex, minimally invasive surgery (MIS) on soft tissues require compactness, dexterity, and responsiveness. These systems frequently have relatively high speed, low stiffness, and highly back-drivable mechanisms,[6].

Many early medical robots were essentially modified industrial robots. This approach has many advantages, including low cost, high reliability, and shortened development times. If suitable modifications are made to ensure safety and sterility, such systems can be very successful clinically. They can also be invaluable for rapid prototyping and research use.

However, the specialized requirements of surgical applications have tended to encourage more specialized designs. For example, laparoscopic surgery and percutaneous needle placement procedures typically involve the passage or manipulation of instruments about a common entry point into the patient's body. There are two basic design approaches. The first approach uses a passive wrist to allow the instrument to pivot about the insertion point and has been used in the commercial Aesop and Zeus robots as well as several research systems. The second approach mechanically constrains the motion of the surgical tool to rotate about Remote Center of Motion (RCM) distal to the robot's structure. In

surgery, the robot is positioned so that the (RCM) point coincides with the entry point into the patient's body. This approach has been used by the commercially developed da Vinci robot, as well as by numerous research groups, using a variety of kinematic designs.

1.5 Types of Medical Robots

The medical robot is categorized into surgical robotics and non surgical, see Figure (1.1).The surgical robotics are used widely because they can improve precision, filter human motion tremor, extend human reach into the body, and reduce the risk of infection. The surgical robots can be divided into Telemanipulators and Image guided robots. Both types of surgical robots allow the surgeon to operate freely in the safe zone, but prevent entry elsewhere and give many dependability: safety, reliability, maintainability and availability,[7].

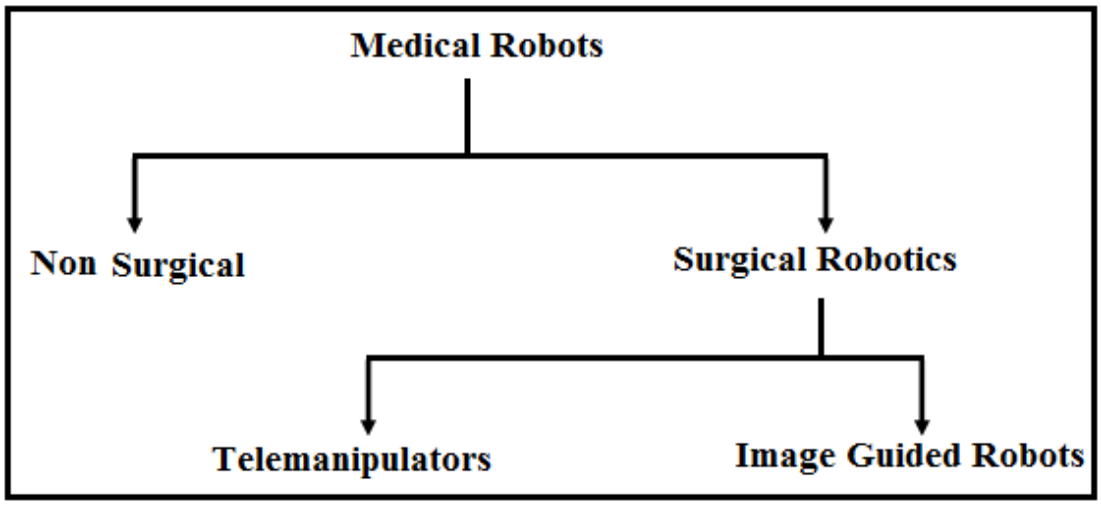

Figure (1.1) Subdivisions Types of Medical Robots,[7]

1.6 Laparoscopic Surgery

Laparoscopic surgery is a revolutionary technique. It is minimally invasive, i.e., the surgery is performed with instruments inserted through small incisions (less than 10 mm in diameter) rather than by making a large incision to expose the operation site. The main advantage of this technique is the reduced trauma to healthy tissue, which is the major

reason for post-operational pain and long hospital stay of the patient. The hospital stay and rest periods, and therefore the procedures' cost, are significantly reduced with minimally invasive surgery, at the expense of more difficult techniques performed by the surgeon.

In less than a decade, there was a quick shift from open surgery to laparoscopic surgery in relatively simple procedures, with 67% of cholecystectomies performed laparoscopically in the USA. Adoption of laparoscopic techniques has been slower in more complex procedures, largely because of the greater difficulty due to the surgeon's reduced dexterity and perception.

In laparoscopic surgery, the abdominal cavity, which is expanded by pumping carbon dioxide inside to open a workspace, is observed with a laparoscope inserted through one of the incisions. Laparoscopes have fiber-optic channels to carry light to illuminate the abdominal cavity, and lens optics to transmit the images. A CCD camera is connected at the outer end of the laparoscope, and the monoscopic image of the operation site is displayed on a high resolution TV display,[8].

In laparoscopy a pneumoperitoneum is created which means that the body cavity is inflated (8–12 mmHg) with carbon dioxide to create workspace. In thoracoscopy a lung is deflated which is sometimes supported with some additional gas. Plastic or metal cannulas (called trocars in the remainder of this thesis) with seals are placed in the incisions to protect the tissue, to simplify exchange of instruments and to keep the carbon dioxide inside the cavity. However, feedback on applied forces is limited due to friction between instruments and seals and can change during one procedure as the instrument becomes more wetted [9].

1.7 Tools of Laparoscopic Surgery

The tools of laparoscopic are so much. However the following main tools are used as shown in Figure (1.2), [10] :

(i) Telescope: This endoscope is made of surgical stainless steel containing an optical lens. The eyepiece, or ocular lens, remains outside of the patient's body and attaches to a camera to view the images on a video monitor. Telescopes or laparoscopes come in various sizes 10 mm or 5mm, 2-3mm 'needlescopes'.

(ii) Trocars: The basic laparoscopic port consists of an outer hollow sheath or cannula that has a valve to prevent the CO_2 gas from escaping, and a side port for instillation of gas. Trocars are available in various diameters and sizes according to requirements, 10mm and 5 mm being commonly used. Disposable rubber converters or reusable metallic reducing sheath are available for reusable trocars to prevent air leakage from the cannula when smaller diameter instruments are used.

(iii) Forceps: Grasping forceps are used for holding and haemostasis and dissection (Endo-Grasp). The handles have a ratchet mechanism for locking onto the tissues to prevent fatigue when the surgeon holds the tissues for a long time.

(iv) Scissors: There are a variety of scissors for dissecting, mobilizing and cutting tissues, which include straight and curved types (Endo Shears).

(v) Needle drivers: A number of laparoscopic needle holders have been designed for laparoscopic suturing with spring loaded mechanisms. Their advantages include easy introduction, atraumatic needle manipulation, good security and easy accurate needle placement.

Disadvantage is that it is difficult to manipulate the thickness of tissue through with needle passes.

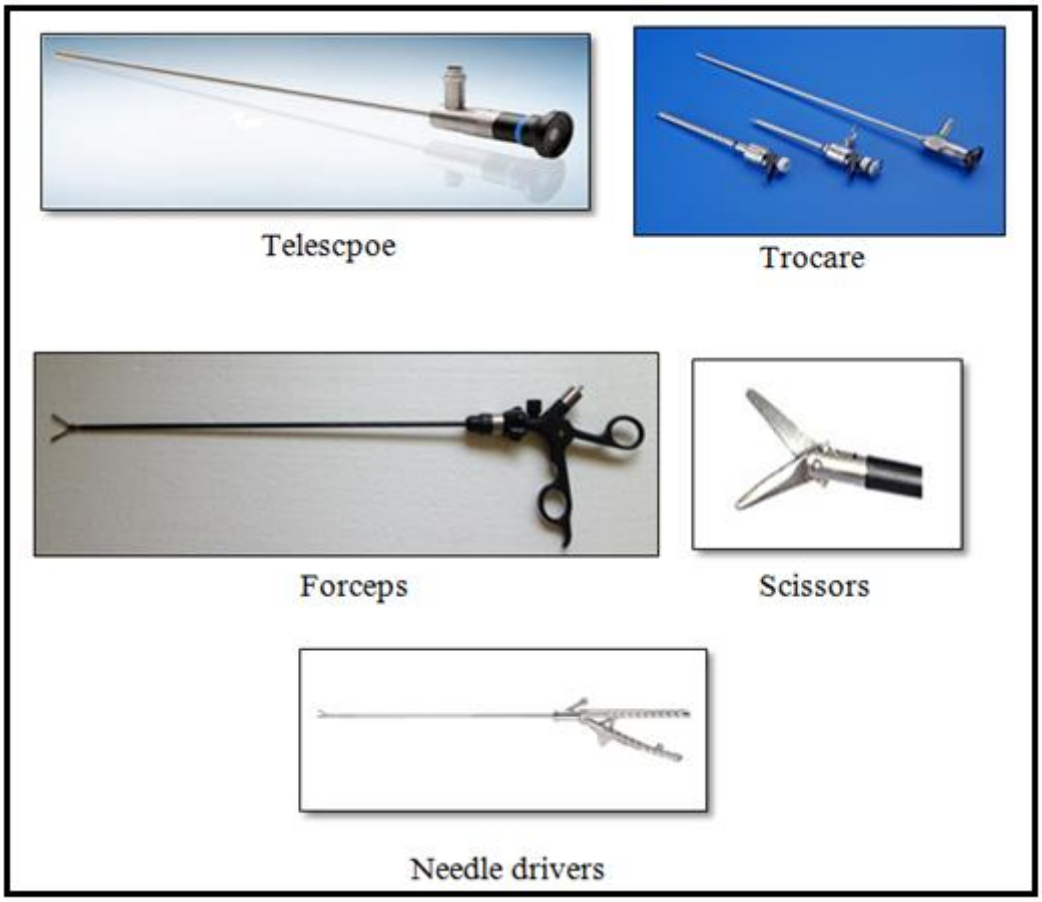

Figure (1.2) The Main Tools of Laparoscopic Surgery,[10]

1.8 Control Surgical System

A control robotic surgical system offers the highest level of automation. It does require a significant amount of preparation to set up to perform each surgery. A specific set of commands, unique to both the patient and the procedure being performed, is first entered into the system by the surgeon and support team. This is accomplished with extensive mapping of the body using medical imaging. Just prior to the surgery, the system is then registered to match the patient's body to the mapping in the surgical system. Finally, the surgery begins. Once the surgery is under way, the robotic system will automatically execute the procedure. The

surgeon will observe the procedure intently and intervene only if necessary,[11].

1.9 Optimization Method

In order to reach to optimal path planning for end effector for manipulator. Path planning consists of finding a sequence of moves for rearranging the robot in a certain environment. The robot occupies certain position in the environment initially. The task is to move the robot to the given goal positions. The robot must avoid obstacles in the environment [12].There are many approaches suggested by researchers to solve the path planning problems of robots in presence of static and moving obstacles based on soft computing. Soft computing consists of fuzzy logic, neural networks and genetic algorithms. Genetic algorithms (GA) require no derivative information or formal initial estimates of the solution, and because they are stochastic in nature. They are capable of searching the entire solution space with more likelihood of finding the global optimum, [13].

Genetic algorithms **(GAS)** are search algorithms and optimization techniques using the principles of natural selection inspired by Darwin's theory about evolution. It is a randomized search algorithm based on biological evolution in nature. It includes the steps of selection, crossover, mutation, and so on. GA is reliable and adaptive. So it is successfully used in the function optimization,[14].

GA repeatedly modify during successive generations a population of different sub-optimal solutions of a given problem. The selection process persists in keeping a number of individuals of the current generation, depending on some criteria, and produces children for the next generation. Over successive generations, the population evolves toward an optimal solution.

The fitness function evaluates, for a given solution, its degree of optimality; the evaluation of this function is essential to the selection process. The fitness must not to be mistaken for the objective function, [15].

1.10 Mechanical Configuration of Laparoscopic Surgery

In laparoscopic surgery, at least four DOFs are required for forceps motion: axial rotation and longitudinal translation of the forceps, and pivot motion around the incision hole on the abdomen Figure (1.3). We realize only four DOFs because redundancy may disturb the miniaturization and simplification of mechanism; those are important factors for clinical application and commercialization. The compact forceps manipulator we have developed consists of two mechanical subcomponents; Friction Wheel Mechanism (FWM) and Gimbals mechanism. The FWM provides axial rotation and longitudinal translation of forceps using friction drive mechanism. Gimbals mechanism realizes pivot motion of forceps. The prototype is shown in Figure (1.4). Dimensions of manipulator are 80×150×320 mm^3 and weight is1.7 kg, [16].

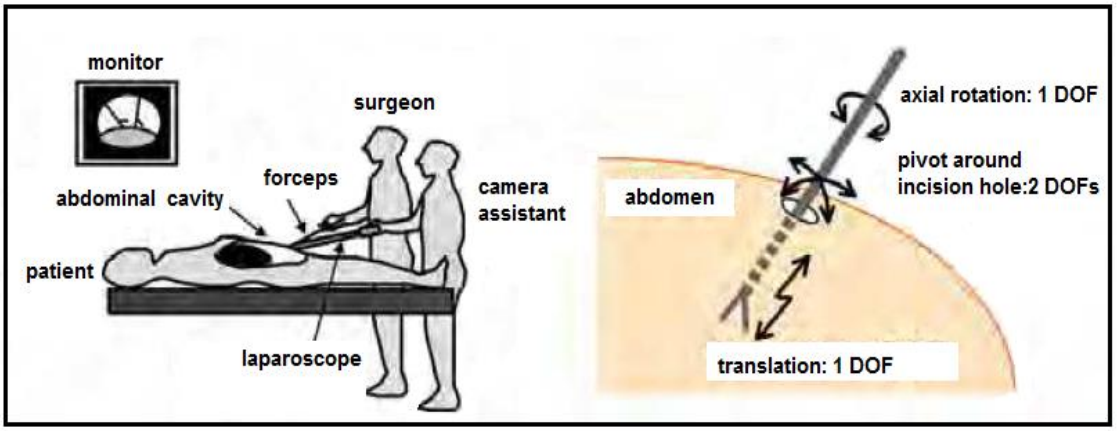

Figure (1.3) Laparoscopic surgery; surgeon manipulates forceps watching video from laparoscope controlled by camera assistant. (left). Limitation of degrees of freedom (rotation, translation, and pivot) is one of causes that make laparoscopic surgery difficult for surgeon(right), [16].

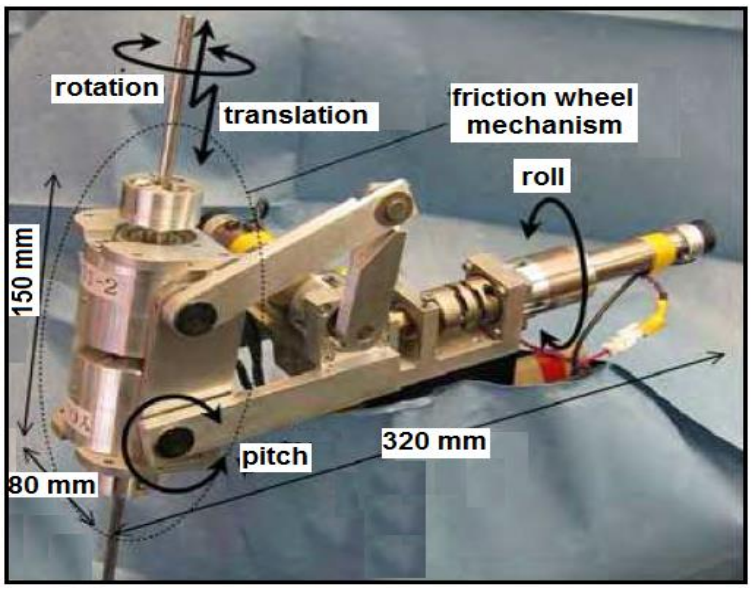

Figure (1.4): Prototype of compact forceps manipulator; friction wheel mechanism provides rotation and translation of forceps, gimbals mechanism realizes pivot motion (roll, pitch), [16].

1.11 Objectives of The Present Work

The main objectives of the work are the experimental and theoretical investigations to: identify the sequences of steps and type of methods necessary to implement a path planning for medical robot (Laparoscope). Seven degree of freedom are achieved by using Genetic Algorithm method (GA) to give the optimal path planning when moving the manipulator from initial point to goal point according to a given workspace. All theoretical results can be matched with experimental results. Studying the control of laparoscope entrance force when surgical instrument through a trocar placed should be taken in experimental work.

Another objective is to study the new gripper design with parallel motion of grasper jaws. To be able to observe tissue blood flow without any damage to the tissue. This depends on the Capillary Pressure values on the tissue.

1.12 Layout of the Present Work

This thesis is organized in the following manner. In Chapter one, is related to introduction of this work. Chapter two includes literature review of previous researches supporting this work. Chapter three includes the theoretical analysis of selected model of seven degrees of freedom surgical robot (laparoscope). It includes the kinematics and dynamics analysis, optimizing performance of laparoscopy and force control entrance laparoscope.

Chapter four contains the optimization path planning using genetic algorithm and experimental work, description of genetic presentation and experimental procedure. Chapter five includes the results obtained from both theoretical and experimental work and discuss these results. Chapter six reports the conclusions of the work and gives some recommendations for future work. In the last section of the presentation the appendices are included.

CHAPTER TWO

LITERATURE REVIEW

2.1 Introduction

In 1985 a robot, the PUMA 560, was used to place a needle for a brain biopsy using CT guidance. Three years later the same machine was used to perform a transurethral resection. In 1987 robotics were used in the first Laparoscopic surgery, a cholescystecotomy. In 1988, The robot, developed at Imperial College London, was used to perform prostatic surgery,[17].

There are several works in the last few years, which are related to determining the optimal trocar position and pose selection of the laparoscopy in minimally invasive surgery (MIS),[18].

2.2 Medical Robot for Surgery of Multi Degree of Freedom

Yun, et al (2003) [19], described the development of a 3-DOF laparoscopic assistant robot system with motor-controlled bending and zooming mechanisms using the voice command motion control and auto-tracking control. The system is designed with two major criteria: safety and adaptability. To satisfy the safety criteria we designed the robot with optimized range of motion. For adaptability, the robot is designed with compact size to minimize interference with the staffs in the operating room. The required external motions were replaced by the bending mechanism within the abdomen using flexible laparoscope. The zooming of the robot is achieved through in and out motion at the port where the laparoscope is inserted. The robot is attachable to the bedside using a conventional laparoscope holder with multiple DOF joints and is compact

enough for hand-carry. The voice-controlled command input and auto-tracking control is expected to enhance the overall performance of the system while reducing the control load imposed on the surgeon during a laparoscopic surgery. The proposed system is expected to have sufficient safety features and an easy-to-use interface to enhance the overall performance of current laparoscopy.

Shyam , et al (2005) [20], presented a new design for a high accuracy, 3-degrees of freedom (DOF) MEMS manipulator. The 3- DOF robotic manipulator is to be used for biomedical applications such as cell probing, tissue sampling, neuron signal reading and drug delivery, in which high accuracy and repeatability of positioning is required. While sensing or imaging elements are not available in the integration with the manipulator to provide feedback for positioning, they investigated a calibration approach to minimize the positioning errors. In-plane and vertical MEMS thermal actuators are chosen to perform the required tasks. Modeling of the thermal actuators was first studied and the results were match with experimental results.

Christopher and Robert (2007) [21], studied that the force feedback may provide additional information that improves performance. A two-handed, six degrees of freedom, endoscopically guided, minimally invasive cannulation task (inserting one tube into another tube) to test this hypothesis, used subjects both trained and untrained in minimally invasive surgery. Their results suggest that force feedback reduce applied forces for both subject groups, but only the surgically trained group can take advantage of this benefit without a significant increase in trial time.

Pisla, et al. (2011) [22], presented the parallel hybrid robot, PARASURG 5M with five degrees of freedom, having the possibility of attaching at its ends either a laparoscope or an active surgical instrument for cutting/grasping, PARASIM, with four degrees of freedom, based on

mathematical modeling. Conclusion of this work has a hybrid parallel, lightweight and simple structure for minimally invasive surgery. The robot is part of the surgical robotic system, PARAMIS, with three arms, one used as a laparoscope holder, and other two for manipulating active instruments, see Figure (2.1).

Figure (2.1) The Experimental Model of PARAMIS, [22]

Taoming (2011) [23], used in his work a 3- DOF robotic wrist mechanism with force feedback for a robotic surgery system. This prototype solves the problem of limited dexterity of traditional surgical tools in MIS caused by small incision acting as a fulcrum. The prototype improves dexterity by integrating a 2- DOF wrist on the instrument tip.

Another problem of the current surgical tools in MIS is that they cannot provide force feedback from the instrument/tissue interaction. Integrated with a 6 axis force/torque sensor, the designed instrument can provide accurate force and torque measurements on the instrument tip during instrument/tissue interaction. The shaft has an 8 mm diameter shaft. The 3- DOF instrument can roll $\pm 360^{o}$, pitch $\pm 90^{o}$, and yaw $\pm 35^{o}$, hence the workspace of the end-effector is a semisphere. The gripper can provide 5.5 N gripping force. The diameter of the gripper is approximately 6.10 mm, its length is 32.3 mm and its weight is 7.3 g. The

angle of gripper jaw opening is 45^{o}. The end-effector can be easily replaced by different surgical tools depending on task being performed.

Duck , et al (2013) [24], proposed a laparoscopic surgery system by using a robot that solves many problems. Among these, its inability in delivering touching sensation to a surgeon is raised as the biggest problem. This paper attempted to find a force feedback controlling method at the time of performing movement by using one-degree of freedom (DOF) arm of slave and master system that is used in the programming based system. The study used force sensors and otherwise, conducted for the force feedback control by using a force sensor and for the case when the sensor could not be used due to the spatial and systematic limitation. The realization of force feedback system was successful, and the experiment results of force feedback control and current based force feedback control mode based on the force sensors of one-DOF system indicates that it could be directly applied to the another multi-DOF surgical robot system that is currently under the development.

2.3 Medical Robot use Intelligent Methods

2.3.1 Fuzzy logic

Ver´onica, et al (2009) [25], proposed a new algorithm for collision handling between 3D agents in a laparoscopic surgery simulator. The aim of this paper is to present an algorithm for collision handling between 3D deformable (organ) and non-deformable (surgical tool) objects involved in a non-structured interaction scene. The proposed approach obtains the new position of each collided vertex of the organ taking into account two key concepts. First, a parameter which embodies the ongoing state of the scene is obtained making use of both kinematic information of the surgical tool and geometric information of the organ surface that

surrounds the vertex under analysis. Second, three parameters inferred from a feedback fuzzy logic system ponderate the nature of the tool motion with respect to the organ, modeled as penetration/extraction and sliding. Preliminary experimental results show that this solution is able to avoid the interpenetration among the multiple colliding points detected in each simulation step in an efficient, physically and spatially coherent manner**.**

Farzin, et al (2013) [26], this research involved developing a surgical robot assistant using an articulated PUMA robot running on a linear or nonlinear axis. The research concentrated on studying the artificial intelligence based switching computed torque controller to localization of an endoscopic tool. By using Fuzzy Logic Methodology (FLM)to resolve the challenge in nonlinear, uncertain, and noisy systems and this is one of the most important applications of fuzzy logic theory**.**

Results show that the switching artificial nonlinear control algorithm is capable to design a stable controller. For this system, error was used as the performance metric.

Seung, et al (2013) [27], presented an application of intelligent fuzzy PID (proportional-integral-derivative) controllers for the position control of a master-slave configuration laparoscopic surgery robot system. For the slave robot controller, two fuzzy PID control algorithms are implemented: a rule-based fuzzy control algorithm for online PID gain tuning and a learning fuzzy controller to tune the rules in the rule-buffer automatically in an online manner. Two fuzzy controllers are tested for sinusoidal reference motions with various periods and the test results are compared with a conventional PID controller in terms of position control performance. Various performance indices were used for the comparison, including RMS (root mean square) error, steady-state error, IAE (integral of average error), ISE (integral squared error), ITAE (integral time-

weighted absolute error), ITSE (integral of time multiplied by the squared error).The evaluation; shows that the learning fuzzy controller yields the best performance among the three algorithms. Furthermore, the relationship between the scaling gains and the performance could be deduced to construct a comparative tuning algorithm, which enables the scaling gains to be optimally tuned, with less trial and error. Further refinement of the algorithm for enhancing the control performance is under way.

2.3.2 Neural Network

Hermann, et al (2008) [28], showed that tying suture knots is a time-consuming task performed frequently during Minimally Invasive Surgery (MIS). Automating this task could greatly reduce total surgery time for patients. Current solutions to this problem replay manually programmed trajectories. But a more general and robust approach is to use supervised machine learning to smooth surgeon given training trajectories and generalize from them. Results obtained using LSTMRNNs (Long Short-Term Memory) trained by the recent Evolino algorithm (Evolino is a framework for supervised sequence learning that combines neuroe volution of artificial neural networks) show that this approach can significantly increase the efficiency of suture knot tying in MIS over preprogrammed control.

Auranuch, et al (2008) [29], proposed surgical marker pattern recognition and rotation angle determination for surgical navigation application. The objective of this study is to implement a new version of tracking algorithm for marker recognition and orientation by using neural network architecture. A rotation-invariant neural pattern recognition system can recognize a rotated pattern and determine its rotation angle. The tracking system consists of markers which are indifferent patterns.

The rotation-invariant neural network algorithm has to be trained by a certain quantity of 2D-Image data in various angles of rotation. As results the system is able to recognize the specific marker patterns and provide information of their rotation angles.

Auranuch, et al (2009) [30], developed dental implant surgical navigation system based on homogenous transformation algorithms. The previous works are presented in numerous basic research. The methodology of design depends on tool tip calibration, optical marker recognition, and pose determination using neural networks. This paper concerns with tracking path generation system based on fundamental of optical tracking. The homogenous transformation has been calculated in term of kinematics equation among marker relationship. The stereo camera is utilized to retrieve 3D position of different pattern styles of markers. The marker recognition algorithm using neural network method is performed to identify markers. The fundamental relationship among markers are computed to obtain the orientation and translation between the guided path and the instrument's tool tip. The experiment has been demonstrated and performed under prototype model. The method is to work on procedure step by step. The path tracking is executed to observe the accuracy of the system. The result shows that the system can be performed to track path based on beforehand planning.

2.3.3 Genetic Algorithm

Sergiu , et al (2007) [31] , proposed an optimization method for a planar micro parallel robot that uses performance evaluation criteria related to the workspace of micro parallel robot. Furthermore, a genetic algorithm is proposed as the principle optimization tool. The success of this type of algorithm for parallel robots optimization has been demonstrated in various papers.

Papanikolaidia , et al (2013) [32], noticed that during the preoperative planning of robotically assisted laparoscopic surgery, one of the most critical issues for the success of the surgery is the trocar port placement (the special tools which are entering the patient's body) and the placement of the entire robotic system (position and orientation). Suitable placement affects the robot's dexterity, reachability in the surgical field, manipulability and visibility in the workspace which are necessary for the successful outcome of a laparoscopic surgical procedure. Even today, distinguished and experienced surgeons have difficulty solving such problems because of the high redundancy of the robots. The main aim of this study is to propose an approach for suboptimal base placement of the Da Vinci Surgical System, in order to maximize the performance of the robot in the surgical site. An aggregated dexterity measure in surgical points is formulated based on the robot configuration dependent manipulability index. The ADM (aggregated dexterity measure) is used as the objective function for the determination of the best robot base location in order to obtain high dexterity performance in the surgical operation area. A genetic algorithm is used to search for the optimal base location. The results noting that even with different parameters of the Genetic Algorithm, the best configuration and placement of the robot varied slightly, indicating the stability of the proposed method.

Rainer,et al (2003)[33], presented a framework for the optimization of the design of a medical robot to accomplish minimally invasive surgery. Surgical interventions are analysed in terms of workspace and accuracy requirements. As optimization criterion, the minimization of the overall size of the robot is considered since a compact design is important in an overcrowded environment such as the operating room. Stress is laid on the formulation of reasonable measures for manipulability and accuracy which are included in the optimization model as constraints. Furthermore,

a method to allow for insensitive robot setups with respect to registration errors is established. Optimization itself is carried out using genetic algorithms with a subsequent gradient-based method. As a result, the optimal link lengths of a medical robot are determined.

2.4 Optimization of Surgical Robot

Gonchar, et al (2000) [34], used simulations in path planning and motion control for medical robot with six degrees of freedom (DOF) in a given 3D environment. They described briefly the essential features of the developed system and its basic components, including its use for determining the optimum or near optimum configuration of the robot manipulator. Determining the configuration is based on the geometric approach to provide high planning precision. The paper presents the simulation system and its use in robot motion planning.

Louaï, et al (2003) [35], investigated a two-step strategy to optimize the most critical settings of an RMIS intervention, namely, the port placement (incision sites for minimally invasive access) and the pose of the robot (initial configuration of stationary joints). The first step relies on a patient-dependent modeling of the intervention by the surgeon that is transformed into an optimization problem where criteria such as visibility and dexterity serve as a cost function. The second one, referred to as the pose planning problem, aims at guaranteeing a collision-free operation of the robot throughout the intervention, by properly assigning stationary extra flexibility at the beginning of the intervention, under the constraint of ensuring the fixed positions of the minimally invasive port access.

Mitchell, et al (2004) [36], focused in this worked on a bottom-up approach in developing a new class of surgical robot arms. The spherical mechanism is a rotational manipulator with all axes intersecting at the center of the sphere. Locating the rotational center of the mechanism at the MIS port makes this class of mechanism a suitable candidate for the

first two links of a surgical robot for both minimally invasive and open surgery. For optimizing the mechanism structure, the forward and inverse kinematics, as well as the Jacobian matrix, were derived. Using the Jacobian, mechanism isotropy was considered as the performance metric. The workspace of this design covers the entire EDWS and is the optimal design for the next generation of surgical manipulator.

By directly applying in-vivo experimental data from MIS in order to optimize the spherical manipulator a design that maximizes performance and minimizes size has been developed. A pair of prototype manipulators will be developed based on these results.

Rainer, et al (2006) [37], investigated a generic approach to optimize the design of an actuated carrier for the DLR (medical robot) multi-arm surgical system is presented. The carrier is attached to the ceiling of the operating room and provides additional degrees of freedom to the surgical robots with the purpose of automatic, optimal positioning of their bases as well as guaranteeing high stiffness. Standard workspaces of minimally invasive as well as open surgical procedures are considered and optimization criteria are derived. The minimum necessary degrees of freedom of the carrier are obtained as well as the optimal segment dimensions by use of an optimization with genetic algorithms.

Qinjun, et al (2007) [38], concentrated on the designs of a radio frequency ablation medical robot system assisting surgeons effective treatment for patients with liver tumors. Surgery space, clinical operation requirements and optimized mechanical structure of robots requirement, are the key factors in designing a perfectly performing medical robot structure which is suitable for surgeons in their operation environment. The development of this medical robot system contributes to the promotion and popularization of the minimal invasive surgery.

Rugi, et al (2012) [39], focused in this worked on the design and optimization of the robot arm. Based on the considering of the actual requirements of the minimally invasive surgery, incision positioning and instrument positioning mechanisms has been designed, which have seven degrees of freedom and can provide enough workspace for MIS operation. According to the characteristics and actual movement of the surgical robot, the forward and inverse kinematics was also analyzed. Moreover, to make sure the robot has a good dexterity degree and high operable performance, the dexterous index is constructed by using the singular value of the Jacobian matrix and an optimization model was build. The robot's structure parameters were optimized by using sequential quadratic programming.

Wael (2013) [40], studied the effect of trajectory planning method duration time on correct dynamic response selection of six degrees of freedom micro-robot intended for surgery applications using two different methods of trajectory planning with different four duration times (5, 10, 20 and 60 sec). The kinematic equations of motion were obtained using Denavit-Hartemberg parameters representation. The dynamic equations of motion, which are important for the proper design of robot controller, were first derived using the Lagrangian-Euler technique. Then, the required hub torque to move each joint was calculated for the motor selection. The trajectory planning was derived using two different methods of trajectory planning with different four duration times (5, 10, 20 and 60 sec). These methods are the fifth-order polynomial and soft motion trajectory planning.

2.5 Summary

The previous studies contained the improvement for the performance, compactness the overall size and force feedback control of medical surgery robotic, which is multi-degrees of freedom. In previous researches have been used of intelligent method for medical robot which was used neural network method to reduce consuming time during the surgical operation and fuzzy logic method is used to detect and prevent collided vertexes between organ and surgical tool. The genetic algorithm method also used to optimize the placement of port incision and the configuration of stationary joint which give the best performance according to nature of application. In this study seven degree of freedom has been chosen and analyzed the motion and force of grasper parallel jaw. In the current research was employed genetic algorithm to find the path optimization and avoiding the obstacles. The researches in this field are very few so it was chosen genetic algorithm method to serve the idea of the current research.

CHAPTER THREE
MODEL ANALYSIS OF SURGICAL ROBOT

3.1 Introduction

Minimally invasive surgery (MIS) or laparoscopy typically involves the use of special surgical instruments with an observation of the surgical field through an endoscope. Each instrument passes through a trocar, a cylinder with a pointed blade end, inserted in the patient's body to make an incision. It is common to insert two instruments and an endoscope at a time through three incisions made on the vertices of a triangle. In single-access MIS, the instruments and the endoscope are inserted through a single incision. MIS causes less operative trauma for the patient than an equivalent invasive procedure (open surgery). It leaves patients with less pain and scarring, speeds recovery, and reduces the incidence of post-surgical complications [41].

3.2 Laparoscopic Procedures and Instruments

Laparoscopic procedures involve insufflations (blowing) CO_2 gas to a pressure of 12-15mmHg into the abdominal cavity. An incision is made on the abdomen, and a 5-10 mm diameter straight trocar (a device used to insert a cannula – an instrument with a hollow barrel through the center) and sleeve are then inserted into the abdominal cavity. A telescope connected by a light cord and camera are used to visualize the operative field on a colored monitor. Laparoscopic instruments are placed through two or more additional trocar sleeves for manipulation by the surgeon,[42].

Generally, laparoscopic instruments are 5mm or 10mm in diameter and 32cm or 45cm in length. The longer-length instruments are used on bariatric (obesity-related) procedures and/or larger size patients. Handles

come in either locking and unlocking, ratcheted or non-ratcheted, insulated or non-insulated designs, and may feature ring handles or other ergonomic designs and materials as preferred by the surgeon.

Conventional instruments used in Minimally Invasive Surgery (MIS) are hand-held instruments with long shafts, an end-effector (needle holder, dissector etc.) at one end and a handle at the other. The instrument passes through the trocar and is effectively constrained by a pivot point. At the pivot point, the instrument motion is constrained to 4 degrees of freedom (DOF) with a reduced range of motion [43].

3.3 Model of The Surgical Robot (Laparoscopic Surgery)

The aim of this thesis is development of the surgical robot (Laparoscopic Surgery) in Iraq hospitals in AL SADER education hospital in MYSAN governorate made by KARL STORZ company. The researcher has visited the hospital and saw all the details of laparoscopic surgery system shown clear in Figures (3.1) and (3.2) and the information given in Table (3-1).

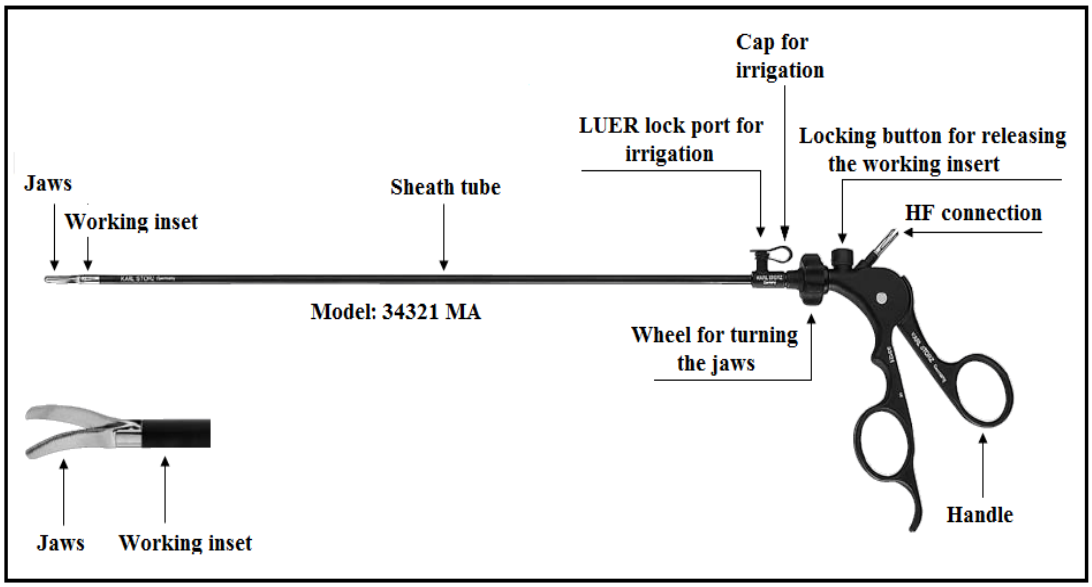

Figure (3.1) The laparoscope in Al Sader Education Hospital, Size 5 mm, Length 36 cm [44].

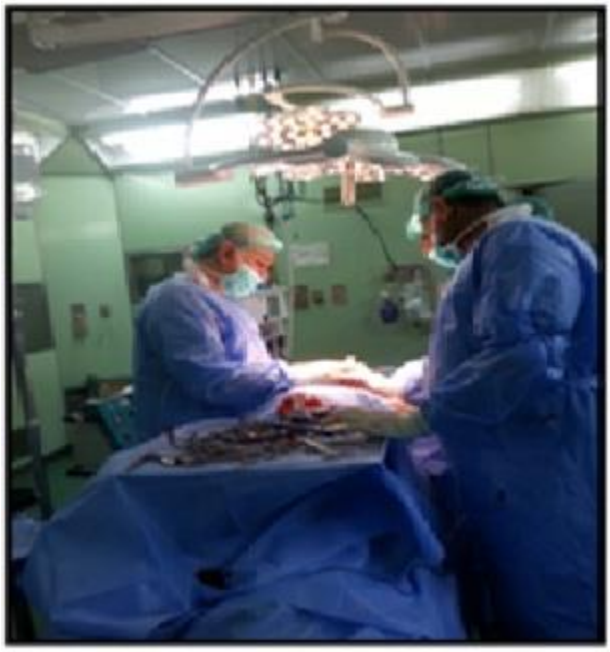

Figure (3.2) Surgeon In Surgical Room In Al Sader Education Hospital

Table (3-1) Laparoscopic Forceps - KARL STORZ,Model 34321 MA,[42].

Product Name	Description
KARL STORZ Design Handle	rotating, dismantling, insulated, with connector pin for unipolar coagulation, length of jaws 20 mm, serrated, spoon-shaped jaws, curved, size 5 mm, length 36 cm
Three Parts Dismentle Structure	-
Types of Jaws	Many types for different operation function for customer demand as shown in appendix (A)
Size Diameter	3.5mm, 5mm, 10mm
Working Length	360mm , 400mm , 450mm
Materials	Stainless steel for shaft, Plastic for knob and handle
Plug for LUER-Lock	connector for cleaning, black, autoclavable

3.4 Kinematics Analysis of Surgical Robot (Laparoscopic)

The surgical robot under consideration has seven DOF and a redundant one for tool replacement. The end effector has 3 rotations Roll, Pitch and Yaw as shown in Figure (3.3). The kinematics analysis for the robot is performed using the Denavvit- Hartenberg representation. A schematic diagram assigning all the joint axes is represented in Figure (3.4) as well.

The seven DOF are:

(1) rotation around the shaft of the instrument,

(2) rotation up and down

(3) rotation left and right about rotational axis

(4) translation along the shaft of the instrument, (5) , (6) and (7) rotation roll , pitch and yaw,[45].

The seven DOF manipulator kinematic parameters are derived using Denavit- Hartemberg formulation shown in Table (3-2).

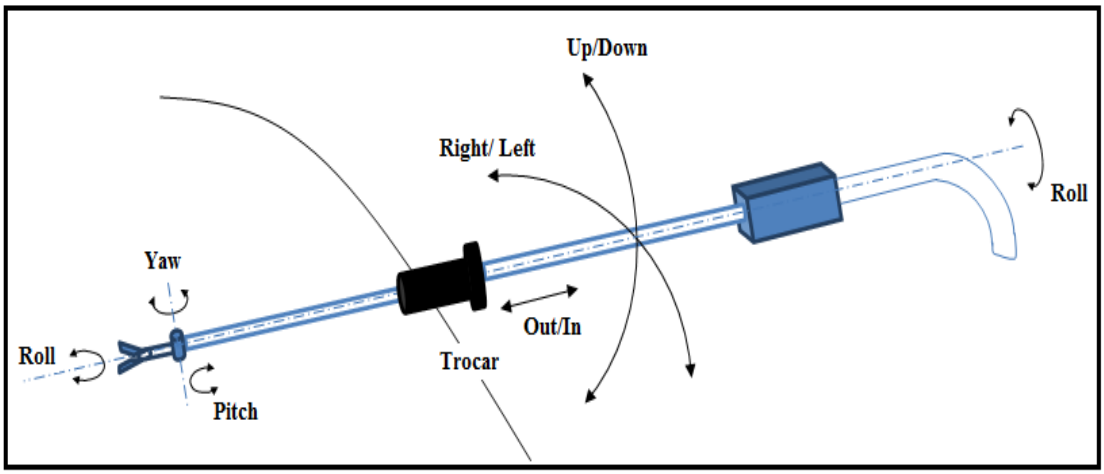

Figure (3.3) A Simulated Laparoscopic with a Seven Degrees of Freedom

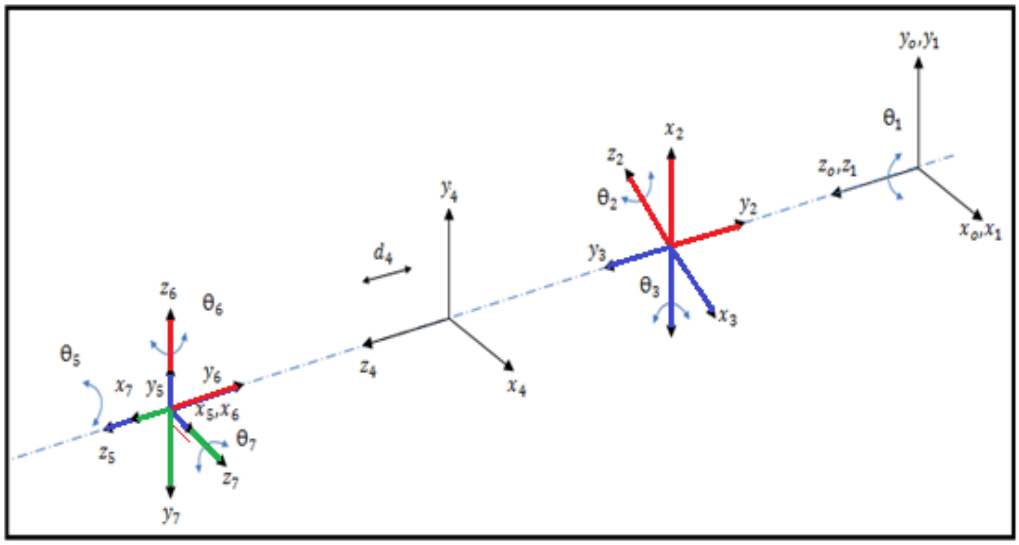

Figure (3.4) All Frames of Manipulator

Table (3-2): Denavit-Hartenberg Parameters

i	α_{i-1}	a_{i-1}	di	θi
1	0	0	0	θ_1
2	-90	0	L_1	θ_2
3	180	0	0	θ_3
4	-90	0	L_1-d_4	0
5	0	0	L_3	θ_5
6	-90	0	0	θ_6
7	-90	0	0	θ_7

3.4.1 Forward Kinematics

In the forward kinematics for a robot mechanism (laparoscope) in a systematic manner, one should use a suitable kinematic model. Denavit-Hartenberg method uses four parameters, $a_{(i-1)}$ –link length, $\alpha_{(i-1)}$ –link twist, d_i –link offset and θ_i–joint angles. The homogenous transformation

matrix for the model is shown in Figure (3.3) and the frames in Figure (3.4).

$$ {}^{i-1}_{i}T=\begin{bmatrix} c\theta_i & -s\theta_i & 0 & a_{i-1} \\ s\theta_i c\alpha_{i-1} & c\theta_i c\alpha_{i-1} & -s\alpha_{i-1} & -s\alpha_{i-1}d_i \\ s\theta_i s\alpha_{i-1} & c\theta_i s\alpha_{i-1} & c\alpha_{i-1} & c\alpha_{i-1}d_i \\ 0 & 0 & 0 & 1 \end{bmatrix} $$

$$ {}^{0}_{1}T=\begin{bmatrix} c\theta_1 & -s\theta_1 & 0 & 0 \\ s\theta_1 & c\theta_1 & 0 & 0 \\ 0 & 0 & 1 & 0 \\ 0 & 0 & 0 & 1 \end{bmatrix} \quad ;{}^{1}_{2}T=\begin{bmatrix} c\theta_2 & -s\theta_2 & 0 & 0 \\ 0 & 0 & 1 & l_1 \\ -s\theta_2 & -c\theta_2 & 0 & 0 \\ 0 & 0 & 0 & 1 \end{bmatrix} $$

$$ {}^{2}_{3}T=\begin{bmatrix} c\theta_3 & -s\theta_3 & 0 & 0 \\ -s\theta_3 & -c\theta_3 & 0 & 0 \\ 0 & 0 & -1 & 0 \\ 0 & 0 & 0 & 1 \end{bmatrix} \quad ;{}^{3}_{4}T=\begin{bmatrix} 1 & 0 & 0 & 0 \\ 0 & 0 & 1 & l_2-d_4 \\ 0 & -1 & 0 & 0 \\ 0 & 0 & 0 & 1 \end{bmatrix} $$

$$ {}^{4}_{5}T=\begin{bmatrix} c\theta_5 & -s\theta_5 & 0 & 0 \\ s\theta_5 & c\theta_5 & 0 & 0 \\ 0 & 0 & 1 & l_3 \\ 0 & 0 & 0 & 1 \end{bmatrix} \quad ;{}^{5}_{6}T=\begin{bmatrix} c\theta_6 & -s\theta_6 & 0 & 0 \\ 0 & 0 & 1 & 0 \\ -s\theta_6 & -c\theta_6 & 0 & 0 \\ 0 & 0 & 0 & 1 \end{bmatrix} $$

$$ {}^{6}_{7}T=\begin{bmatrix} c\theta_7 & -s\theta_7 & 0 & 0 \\ 0 & 0 & 1 & 0 \\ -s\theta_7 & -c\theta_7 & 0 & 0 \\ 0 & 0 & 0 & 1 \end{bmatrix} $$

The forward kinematics are from the base, Frame (0) to the tip of end-effector frame (7) .

$$^{base}_{end-effector}T = {}^{0}_{7}T = {}^{0}_{1}T\ {}^{1}_{2}T\ {}^{2}_{3}T\ {}^{3}_{4}T\ {}^{4}_{5}T\ {}^{5}_{6}T\ {}^{6}_{7}T$$

$$^{0}_{7}T = \begin{bmatrix} r_{11} & r_{12} & r_{13} & p_x \\ r_{21} & r_{22} & r_{23} & p_y \\ r_{31} & r_{32} & r_{33} & p_z \\ 0 & 0 & 0 & 1 \end{bmatrix}$$

$r_{11} = c_3\,(c_5\,c_6\,c_7 + s_5\,s_7) + s_3\,(c_6\,c_7)$

$r_{12} = c_3\,(-c_5\,c_6\,c_7 + s_5\,c_7) - s_3\,(s_6\,s_7)$

$r_{13} = c_3\,(-c_5\,s_6) + s_3\,c_6$

$p_x = -s_3\,(L_3 + L_2 - d_4)$ …..(3.1)

$r_{21} = -s_3\,(c_5\,c_6\,c_7 + s_5\,s_7) + c_3\,(s_6\,s_7)$

$r_{22} = -s_3\,(-c_5\,c_6\,s_7 + s_5\,c_7) - c_3\,(s_6\,s_7)$

$r_{23} = s_3\,(c_5\,s_6) + c_3\,c_6$

$p_y = -c_3\,(L_3 + L_2 - d_4)$ …..(3.2)

$r_{31} = s_5\,c_6\,c_7 - s_7 c_5$

$r_{32} = -c_6\,s_7\,s_5 - c_7\,c_5$

$r_{33} = -s_5\,s_6$

$p_z = 0$ …..(3.3)

3.4.2 Inverse Kinematics

It is needed in the control of manipulator, to solve the inverse kinematics this to computationally expansive and generally takes a very long time control of manipulators. The conversion of the position and

orientation (H.T matrix) of a manipulator end-effector from Cartesian space to joint space is called inverse kinematics problem.

In this thesis using Algebraic solution approach was used. That is to determine the value of angle (θ_1) and distance (d_4). All details of inverse kinematics analysis are in appendix (B).

${}^0_7T = {}^0_1T\ {}^1_2T\ {}^2_3T\ {}^3_4T\ {}^4_5T\ {}^5_6T\ {}^6_7T$

$[{}^0_1T\ {}^1_2T\ ]^{-1}\ {}^0_7T = {}^2_3T\ {}^3_4T\ {}^4_5T\ {}^5_6T\ {}^6_7T$

$\theta_1 = A\tan2(-p_x, p_y) \pm (A\tan2(\sqrt{p_x^2 + p_y^2 - L_1^2}, L_1)$ .....(3.4)

$\theta_2 = A\tan2(A, B) \pm (A\tan2(\sqrt{A^2 + B^2 - C^2}, C)$ .....(3.5)

$\theta_{13} = A\tan2(-p_x, -p_y) \pm (A\tan2(\sqrt{p_x^2 + p_y^2 - L_1^2}, L_1)$

$\theta_3 = \theta_{13} - \theta_1$

$d_4 = [L_3 + L_2 - (c_1^2 p_x^2 + 2c_1 p_x p_y s_1 + s_1^2 p_y^2 + p_z^2]^{1/2}$ .....(3.6)

$$c_5 = \frac{-c_1 c_{23} r_{13} + c_2 s_{13} r_{23} + s_2 s_{33}}{s_6}$$

$\theta_5 = A\tan2(\sqrt{1 - c_5^2}, c_5)$ .....(3.7)

$$-s_2 c_{13} r_{13} + s_2 s_{13} r_{23} + c_2 r_{33} = -c_6$$

$\theta_6 = A\tan2(\pm\sqrt{1 - c_6^2}, -c_6)$ .....(3.8)

$$s_7 = \frac{-s_2 c_{13} r_{12} + s_2 s_{13} r_{22} + c_2 r_{32}}{s_6} = C$$

$$c_7 = \sqrt{1 - C^2}$$

$\theta_7 = A\tan2\left(\sqrt{1-c_7{}^2}, c_7\right)$ …..(3.9)

3.5 Velocities And Static Forces of Laparoscope

The Jacobian matrix relates joint velocities to end-effector angular velocities. It can be expressed with respect to any of the frames associated with the mechanism. If the Jacobian is expressed in Frame 5, the eigen value corresponding to the angular velocity of Frame 5 has a value of 1 for all poses and joint velocities.

We can find the linear and angular velocity of end-effector by computing the basic Jacobian [46]:

3.5.1 Angular Velocity and Linear Velocity Propagation

(i) Revolted Joints: Figure (3.5) show revolted and prismatic joints.

$${}^{i}\omega_{i+1} = {}^{i}\omega_{i} + {}^{i}\Omega_{i+1} \quad \text{…..(3.10)}$$

$${}^{i}\Omega_{i+1} = {}^{i}z_{i+1}\left(\dot{\theta}_{i+1}\right) = {}_{i+1}^{i}R.\ {}^{i+1}z_{i+1}\left(\dot{\theta}_{i+1}\right) \quad \text{…..(3.11)}$$

$${}^{i+1}z_{i+1} = \begin{bmatrix}0\\0\\1\end{bmatrix} \quad \text{…..(3.12)}$$

$$\begin{aligned}
{}^{i}\vec{\omega}_{i+1} &= {}^{i}\vec{\omega}_{i} + {}_{i+1}^{i}R\cdot {}^{i+1}\vec{z}_{i+1}\left(\dot{\theta}_{i+1}\right)\\
{}^{i+1}\vec{\omega}_{i+1} &= {}_{i}^{i+1}R\cdot {}^{i}\vec{\omega}_{i} + {}^{i+1}\vec{z}_{i+1}\left(\dot{\theta}_{i+1}\right) = {}_{i}^{i+1}R\cdot {}^{i}\vec{\omega}_{i} + \begin{bmatrix}0 & 0 & 1\end{bmatrix}^{T}\cdot\left(\dot{\theta}_{i+1}\right)
\end{aligned} \quad \text{…..(3.13)}$$

$$\begin{aligned}
{}^{0}\vec{V}_{i+1} &= {}^{0}\vec{V}_{i} + {}^{0}\vec{\Omega}_{i}\times\left({}_{i}^{0}R\,{}^{i}\vec{P}_{i,i+1}\right)\\
\vec{v}_{i+1} &= \vec{v}_{i} + \vec{\omega}_{i}\times\left({}_{i}^{0}R\,{}^{i}\vec{P}_{i,i+1}\right)\\
{}^{i}\vec{v}_{i+1} &= {}^{i}\vec{v}_{i} + {}^{i}\vec{\omega}_{i}\times {}^{i}\vec{P}_{i,i+1}\\
{}^{i+1}\vec{v}_{i+1} &= {}_{i}^{i+1}R\cdot\left({}^{i}\vec{v}_{i} + {}^{i}\vec{\omega}_{i}\times {}^{i}\vec{P}_{i,i+1}\right)
\end{aligned} \quad \text{…..(3.14)}$$

(ii) Prismatic Joint

$$
\begin{aligned}
{}^{i}\vec{\omega}_{i+1} &= {}^{i}\vec{\omega}_{i} \\
{}^{i+1}\vec{\omega}_{i+1} &= {}^{i+1}_{i}R \cdot {}^{i}\vec{\omega}_{i}
\end{aligned}
\qquad \text{.....(3.15)}
$$

$$
\begin{aligned}
\vec{v}_{i+1} &= \vec{v}_{i} + \vec{\omega}_{i} \times \left({}^{0}_{i}R\, {}^{i}\vec{P}_{i,i+1} \right) + {}^{0}_{i+1}R \cdot {}^{i+1}\vec{z}_{i+1}\dot{d}_{i+1} \\
{}^{i}\vec{v}_{i+1} &= {}^{i}\vec{v}_{i} + {}^{i}\vec{\omega}_{i} \times {}^{i}\vec{P}_{i,i+1} + {}^{i}_{i+1}R \cdot {}^{i+1}\vec{z}_{i+1}\dot{d}_{i+1} \\
{}^{i+1}\vec{v}_{i+1} &= {}^{i+1}_{i}R \cdot \left({}^{i}\vec{v}_{i} + {}^{i}\vec{\omega}_{i} \times {}^{i}\vec{P}_{i,i+1} \right) + \begin{bmatrix} 0 & 0 & \dot{d}_{i+1} \end{bmatrix}^{T}
\end{aligned}
$$

.....(3.16)

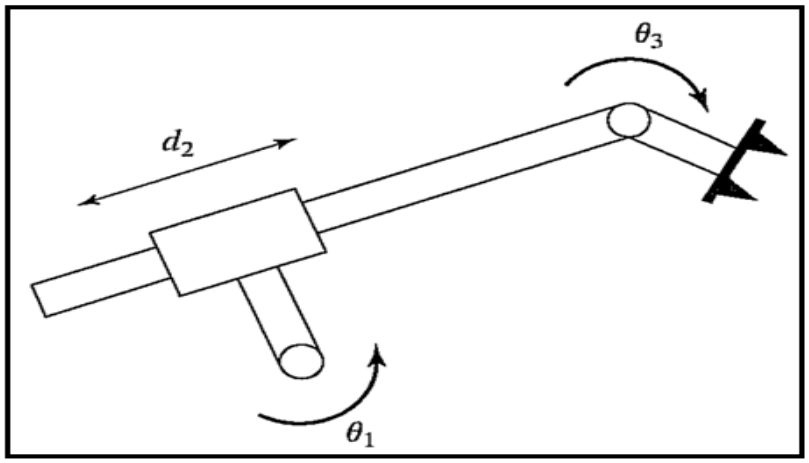

Figure (3.5) The revolted joints and the prismatic joint

$$\dot{X} = J(\theta)\dot{\theta}$$

$$\begin{bmatrix} \dot{x} \\ \dot{y} \\ \dot{z} \\ \omega_x \\ \omega_y \\ \omega_z \end{bmatrix} = J(\theta) \begin{bmatrix} \dot{\theta}_1 \\ \dot{\theta}_2 \\ \dot{\theta}_3 \\ \dot{\theta}_5 \\ \dot{\theta}_6 \\ \dot{\theta}_7 \end{bmatrix} \qquad \text{.....(3.17)}$$

$$J(\theta) = \begin{bmatrix} \frac{\partial h_1}{\partial \theta_1} & \frac{\partial h_1}{\partial \theta_2} & \frac{\partial h_1}{\partial \theta_3} & \frac{\partial h_1}{\partial \theta_5} & \frac{\partial h_1}{\partial \theta_6} & \frac{\partial h_1}{\partial \theta_7} \\ \frac{\partial h_2}{\partial \theta_1} & \frac{\partial h_2}{\partial \theta_2} & \frac{\partial h_2}{\partial \theta_3} & \frac{\partial h_2}{\partial \theta_5} & \frac{\partial h_2}{\partial \theta_6} & \frac{\partial h_2}{\partial \theta_7} \\ \frac{\partial h_3}{\partial \theta_1} & \frac{\partial h_3}{\partial \theta_2} & \frac{\partial h_3}{\partial \theta_3} & \frac{\partial h_3}{\partial \theta_5} & \frac{\partial h_3}{\partial \theta_6} & \frac{\partial h_3}{\partial \theta_7} \\ \frac{\partial h_4}{\partial \theta_1} & \frac{\partial h_4}{\partial \theta_2} & \frac{\partial h_4}{\partial \theta_3} & \frac{\partial h_4}{\partial \theta_5} & \frac{\partial h_4}{\partial \theta_6} & \frac{\partial h_4}{\partial \theta_7} \\ \frac{\partial h_5}{\partial \theta_1} & \frac{\partial h_5}{\partial \theta_2} & \frac{\partial h_5}{\partial \theta_3} & \frac{\partial h_5}{\partial \theta_5} & \frac{\partial h_5}{\partial \theta_6} & \frac{\partial h_5}{\partial \theta_7} \\ \frac{\partial h_6}{\partial \theta_1} & \frac{\partial h_6}{\partial \theta_2} & \frac{\partial h_6}{\partial \theta_3} & \frac{\partial h_6}{\partial \theta_5} & \frac{\partial h_6}{\partial \theta_6} & \frac{\partial h_6}{\partial \theta_7} \end{bmatrix} \qquad \text{.....(3.18)}$$

3.5.2 Static Forces In Manipulators

Another application of the Jacobian is to define the relationship between forces applied at the end-effector and torques needed at the joints to support these forces, [47]. We described the relationship between

linear velocities and angular velocities at the end-effector and the joint velocities.

Here we consider the relationship between end-effector forces and moments as related to joint torques. We will denote by f and n the static force and moment applied by the end-effector to the environment. T_1, T_2, ... , T_n are the torques needed at the joints of the manipulator to produce f and n.

(i) Force Propagation

let:

f_i= force exerted on link i by link (i-1)

n_i = torque exerted on link i by link (i-1)

Joint torques that must be acting to keep the system in static equilibrium, solved as followed:

No net forces, no net torques (moments)

$$\sum f = 0, \qquad \sum n = 0$$

$$^{i}f_{i} = {}^{i}f_{i+1} \qquad \text{.....(3.19)}$$

$$^{i}n_{i} = {}^{i}n_{i+i} + {}^{i}P_{i+1} \text{ X } {}^{i}f_{i+1} \qquad \text{.....(3.20)}$$

Static force propagation from link to link:

$$^{i}f_{i} = {}_{i+1}^{i}R \; {}^{i+1}f_{i+1} \qquad \text{.....(3.21)}$$

$$^{i}n_{i} = {}_{i+1}^{i}R \; {}^{i+1}n_{i+1} + {}^{i}P_{i+1} \; X \; {}^{i}f_{i} \qquad \text{.....(3.22)}$$

(ii) Revolute joint

$$\tau_i = {}^{i}n_i^T \; {}^{i}Z_i \qquad \text{.....(3.23)}$$

(iii) Prismatic joint

$$\tau_i = {}^{i}f_i^{T}\ {}^{i}Z_i \qquad \text{.....(3.24)}$$

3.6 Optimizing Performance of Laparoscopy

Many factors affect laparoscopic working space. The body size cannot be influenced. Other factors such as intra-abdominal carbon dioxide (CO_2) pressure, bowel content, positioning of the patient, and muscle tone can be influenced to increase working space [48]. For suitable working space in laparoscopy are must use laparoscopy tools of good characteristics like (small size, safety for tissues, ……,etc). In this thesis study of Parallel Play of Grasper Jaws is performed.

3.6.1 Parallel Play of Grasper Jaws

Figure (3.6) shows the parallel motion of the grasper jaws with respect to each other. This is important for two reasons; firstly, it allows for equal force distribution across the grasper jaws. Secondly, if the grasper jaws are not parallel to each other when fully closed, it results in a tiny gap at the tip of the grasper jaws, which can impede the user's efforts to grip a thin piece of tissue with the tip of the grasper. Figure (3.7) shows the instruments inside the abdominal cavity.

In this work study and analysis to griper of parallel jaws which depends on design considerations as follows:

(1)-The generated pressure from griper on the tissues be less than damaging limits to the tissues (direct or indirect damage).

(2)-Closed griper diameter will be 5mm or less which allows its entrance and exit from trocar easily.

(3)-It should be efficient and active to give best performance in work space.

(4)- Pressure sensor (the piezoelectric effect pertains to the coupling between pressure and electric charge/field) located in two of the grasper jaws helps surgeons control the pressure applied during grasping see appendix (C), [49].

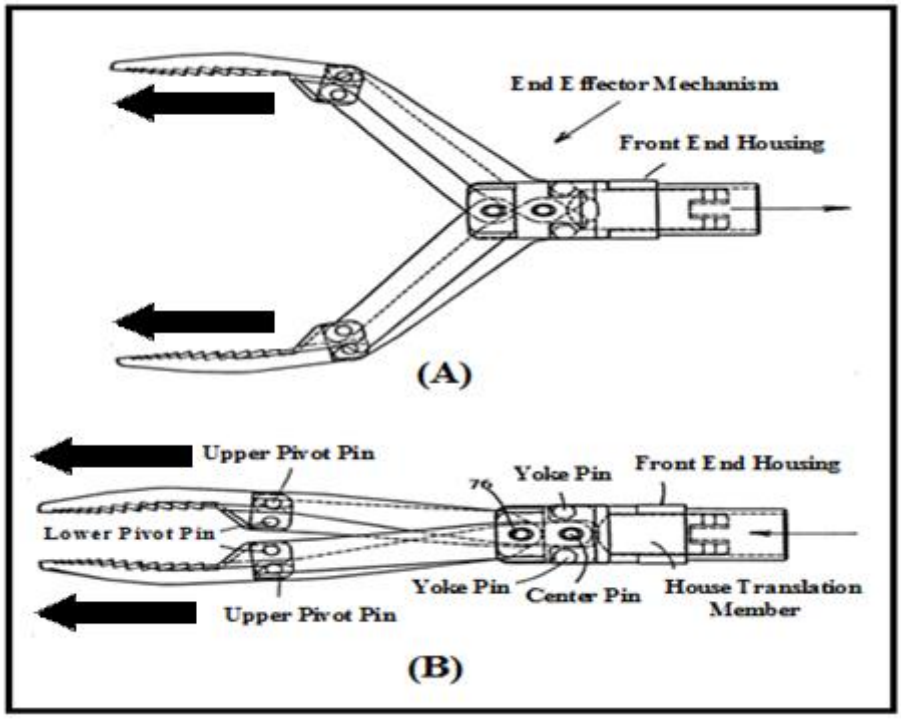

Figure (3.6) (A)- Side Cross-Sectional View with The Jaws Fully Deployed.
(B)- Side Cross-Sectional View with Jaws in a Nearly Closed,[50].

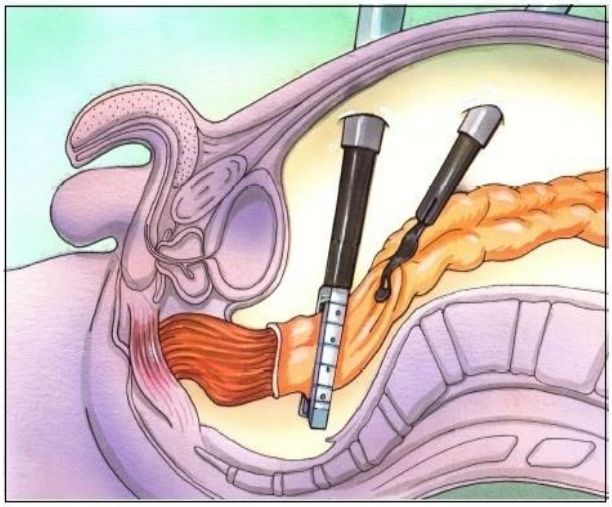

Figure (3.7): The Instruments Inside The Abdominal Cavity,[51].

3.6.2 Analysis of Grasper Forces and Motion

To determine many faces of grasper of jaw motion, it has benefit to easy the connection into separated parts of connections. As shown in Figure (3.8) [52].

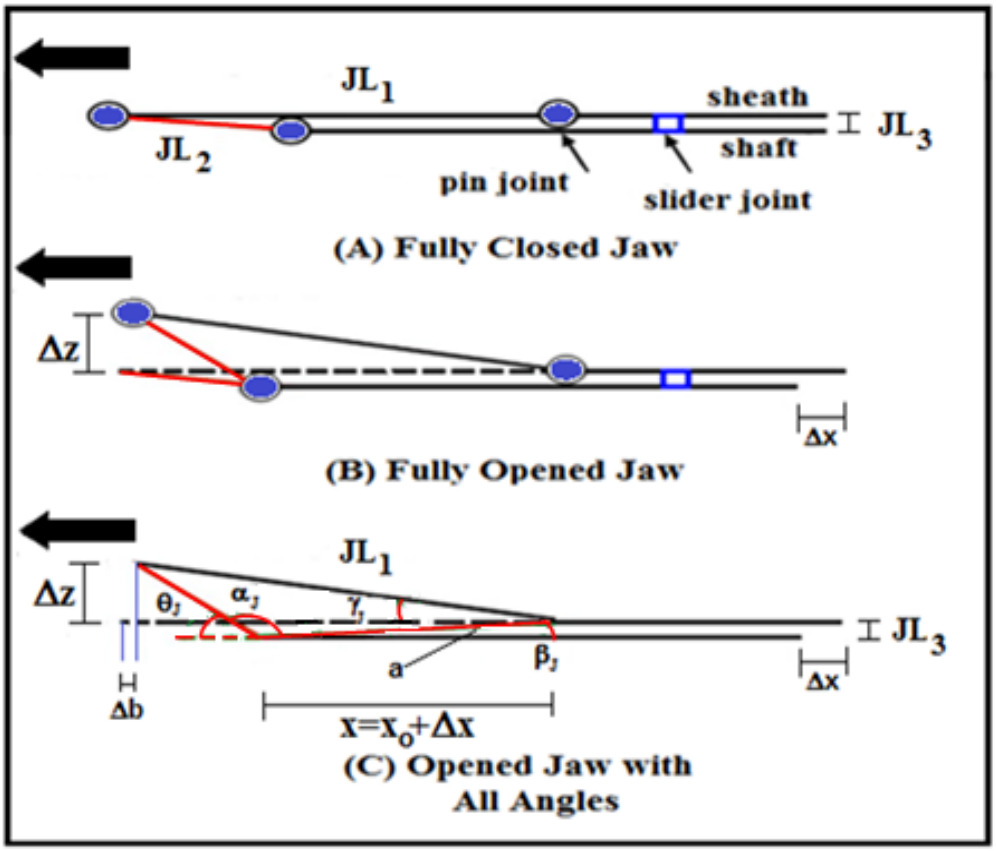

Figure (3.8) The Analytical Method For Jaws Parallel

(i) The Height of Jaw Opening

The height of jaw opening, Δz with respect to the horizontal motion of the shaft, Δx was solved as shown below and in Figure (3.8):

$$a = \sqrt{x^2 + JL_3^2} \qquad .....(3.25)$$

$$\alpha_J = \cos^{-1}\left[\frac{-JL_1^2 + a^2 + JL_2^2}{2.a.JL_2}\right] \qquad .....(3.26)$$

$$\beta_J = \tan^{-1}\frac{JL_3}{x}$$

$$\theta_J = \pi - \alpha - \beta \qquad .....(3.27)$$

$$\Delta Z = JL_2 \sin\theta_J - JL_3 \qquad .....(3.28)$$

(ii) The Horizontal Motion of Grasper Jaws

The link JL_1, shows the front movement of the instrument. The front movement of the rod is inhibited from being switched to the instrument jaws in case of jaw separation.

Figure (3.8) shows a plot of the backward motion, Δb, against Δz_{max}, the maximum jaw opening width, from the equation and in Figure (3.8-C):

$$\sin\gamma_J = \frac{\Delta z_{\max.}}{JL_1}$$

$$\Delta b = JL_1[1-\cos\gamma_J] = JL_1[1-\cos(\sin^{-1}\frac{\Delta z_{\max.}}{JL_1}] \qquad .....(3.29)$$

(iii) The Analysis of Shaft Forces

Figure (3.9) shows the analyzes of forces experienced by the linkages during grasping.

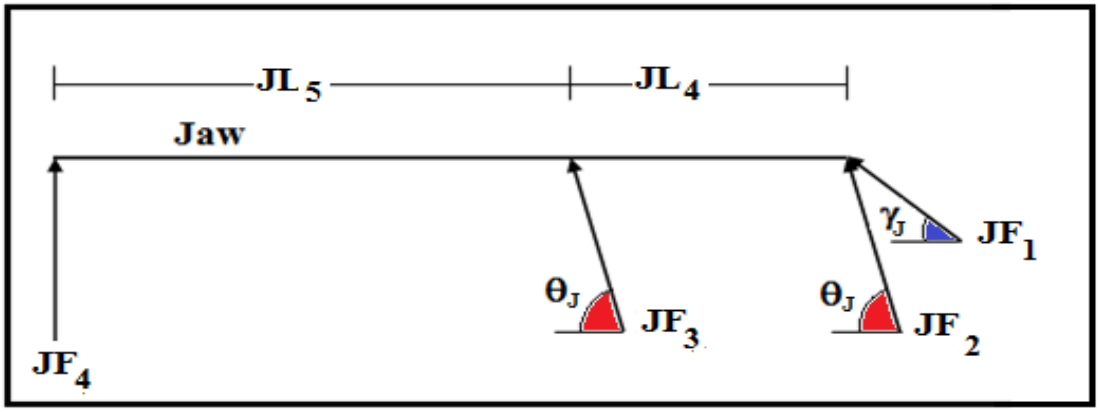

Figure (3.9) Schematic of forces acting on grasper jaw.

By summing the moments about the point at which JF_1 and JF_2 acts on the grasper jaw, JF_3 was solved as

$$JF_3\ JL_4.\sin\theta_J + JF_4(JL_5 + JL_4) = 0$$

$$JF_3 = -\frac{JF_4(JL_5 + JL_4)}{JL_4.\sin\theta_J} \qquad .....(3.30)$$

By summing the force components in the x-direction, an expression of (JF_1) was obtained as:

$$JF_1 = -(JF_2 + JF_3)\frac{\cos\theta_J}{\cos\gamma_J} \qquad ......(3.31)$$

By summing the force components in the z-direction, and substituting the expression for JF_1 in equation (3.31), an expression of JF_2 was obtained as

$$JF_2 = -JF_3 + \frac{JF_4}{\sin\theta_J}(-1 + \frac{\cos\theta_J.\sin\gamma_J}{\sin\theta_J.\cos\gamma_J})^{-1} \qquad ....(3.32)$$

3.7 Control of This Work

Control system has gained significance internationally in the field of surgical procedures. It can increase the stability and robustness of medical procedures. Control relates the dynamic and kinematics of robot to a prescribed motion. The technique of position control based force control has been improved by the complete teleoperated surgical robots where the laparoscope and surgical instruments are moved by the manipulators. The surgeon is directly giving the control signals to the machine through a force sensor. It is possible to read and process these signals in real time to create the robot's motion. Path Planning is a part of control, in which they plan a path followed by the manipulator in a planned time profile. Paths can be planned in joint or Cartesian space. Figure (3.10) depicts the concept of the direct linkage between the control system and the path planning.

This work is clarified by the sequence of these steps:

Step 1: Taking the model of laparoscope (surgical robot) and make the analysis of this model.

Step 2: From the analysis the forward and inverse kinematics gives the position equation which contained control parameters of this model. The forward kinematics gives the constraint of the robot entered to the planning program as explained in chapter four.

Step 3: Inverse kinematics gives the equation for each joint (rotation, prismatic) as explained in this chapter.

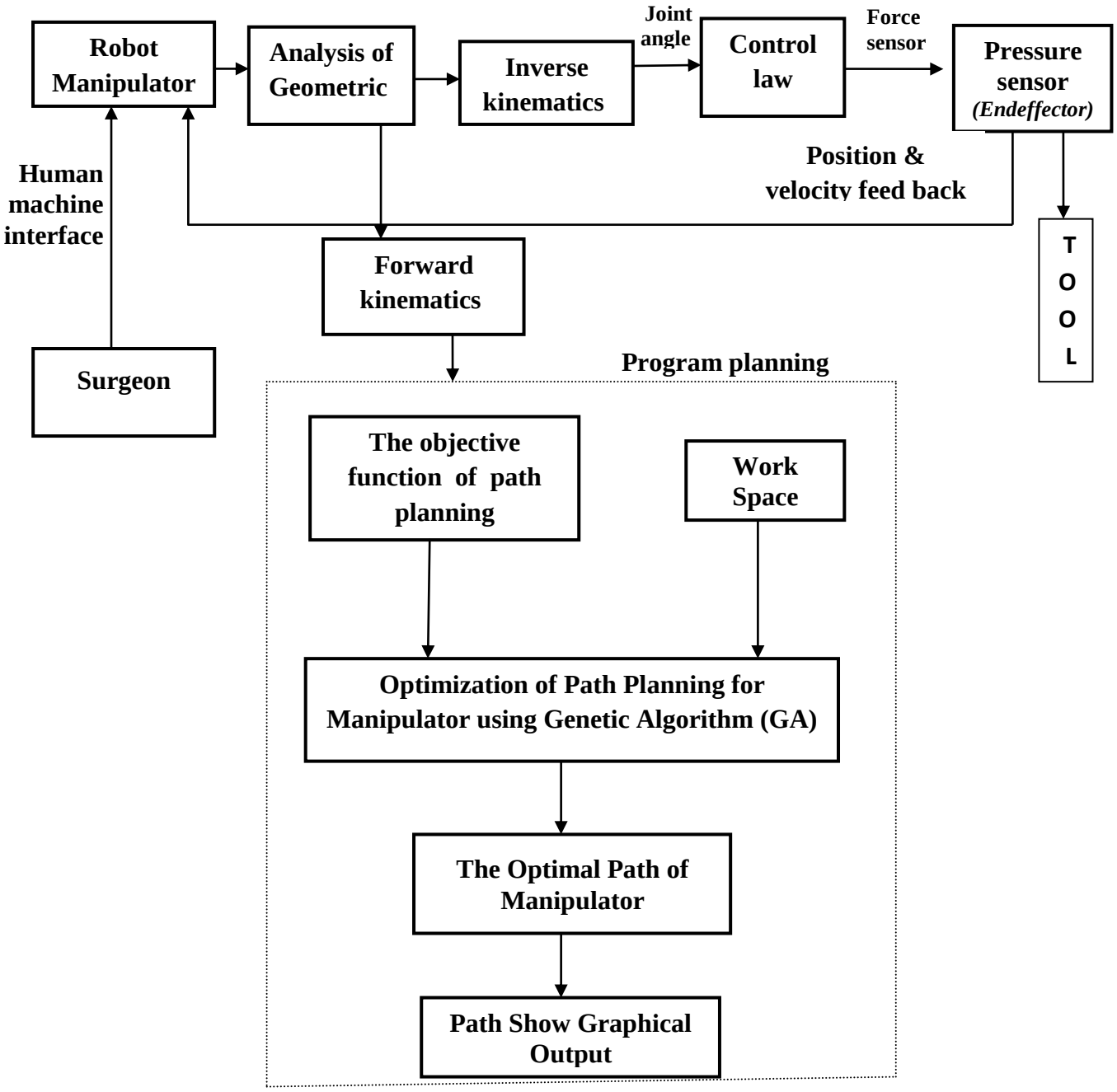

Figure (3.10) Flow Chart of This Work

CHAPTER FOUR

OPTIMIZATION PATH PLANNING USING GENETIC ALGORITHM AND EXPERIMENTAL WORK

4.1 Introduction

A robot is a combined mechanical, electronic, and computer system that follows a simple cycle of commands and task execution for operation. The range of motion of each manipulator is called working space. The instrument with which the robot performs the desired task is attached to the last link of the arm and is referred to as the end-effector, End-effector can be a needle, grasper, scalpel,…etc.[55].

Path planning can be defined as "the determination of a path that a robot must take in order to pass over each point in an environment thus reaching the desired location. The path is a plan of geometric locus of the points in a given space where the robot has to pass through", [56].

Genetic Algorithm was applied to provide optimal path and select the shortest path in predictable environment which will be able to handle static obstacles.

4.2 Optimization of Path Planning

The optimization problems are centered with three factors: an objective function (which is to be minimized or maximized), a set of unknown or variables that affect the objective function. The last factor is a set of constraints that allow the unknowns to take on certain values [57].

The purpose of path planning algorithms is to find a collision free route that satisfies certain optimization parameters between two points [58].

The problem of path planning consists of finding a sequence of moves for rearranging the robot in a certain environment. The robot occupy certain position in the environment initially. The task is to move the robot

to the given goal positions. The robot must avoid obstacles in the environment. The main difficulties for robot path-planning problems are computational complexity, local optimum and adaptability [59].

There are two categories of path planning algorithms: namely the global path planning (off-line) and the local path planning (on-line), based on the availability of information about the environment. Global path planning of robots in environments where complete information about stationary obstacles and trajectory of moving obstacles are known in advance. So the robot only needs to compute the path once at the beginning and then to follow the planned path up to the goal point. When complete information about environment is not available in advance, robot gets information through sensors as it moves through the environment. This is known as on-line or local path planning [60].

To find a path from an actual position of the controlled robot to a desired goal position, while all these parameters stand as the inputs of the algorithm; the output is the optimal path from start to goal [61].

4.3 Genetic Algorithms

The problem to be solved using GA is encoded as a chromosome that consists of several genes. The solution of the problem is represented by a group of chromosomes referred to as a population. In each iteration of the algorithm, the chromosomes in the population will undergo one or more genetic operations such as crossover and mutation. The result of the genetic operations will become the next generations of the solution. This process continues until either the solution is found or a certain termination condition is met. The idea behind GA is to have the chromosomes in the population to slowly converge to an optimal solution. At the same time, the algorithm is supposed to maintain enough diversity so that it can scan a large search space [62].

4.4 Path Planning Optimization Based on Genetic Algorithm

Genetic Algorithms intuitively use randomness to generate a solution in a more intelligent manner than the probabilistic road map method and faster than another path planning methods. GA is capable of generating an optimal (shortest distance) path planning for a robot to visit all the specified way points without colliding with the known obstacles [63].

When using GA's, we need a solution space composed of a set of nodes randomly generated in a free configuration space. The algorithm execution is performed by the research of the best configurations between the initial and the final nodes with checking the optimization criterion which is here the distance. The strength of this method is that it allows to explore and exploit the best solutions by two operators, which are selection and genetic reproduction [64].

GA has shown significant performance compared to other algorithms in term of reliability. GA is a class of stochastic search algorithms based on biological evolution. It does not require derivative information; it can provide a list of optimum parameters, not just a single solution. Considering these facts, robot path optimization can be performed effectively with GA because the algorithm performs a parallel, but directed search to evolve the most fitted solution in a systematic approach [65].

Figure (4.1) depicts a framework to represent Path Planning. As shown, a model of the map of robot workspace area including the location of robot, obstacles and free space area known as configuration space, must first be created. In configuration space, all possible configurations of robot are represented. Then, the configuration space will be modeled by defining the free space area to construct a graph that represents the connectivity of the space. This graph is constructed by

using an appropriate algorithm that presents the connectivity of the graph which also known as graph search optimal path using GA. Finally, the Path Planning algorithm is applied within this graph to find a feasible path for the robot to reach the goal.

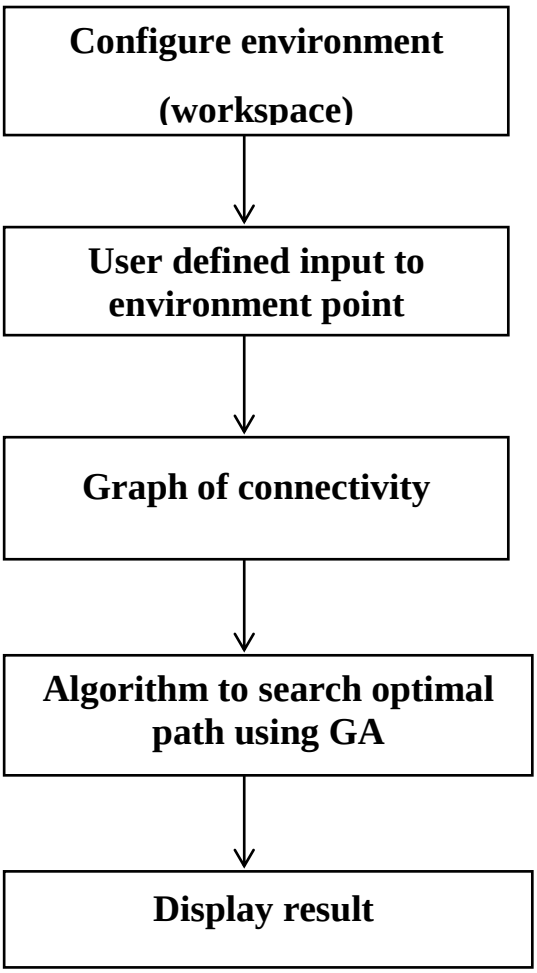

Figure (4.1) The Framework To Find Optimal Path

4.5 Genetic Representation

This section explains the details of the internal structure of the GA and describes its implementation which is represented in the flowchart of GA Figure (4.2).

To evaluate the operation of GA the performance of the following parameters must be calculated:

(i) Initialization

We must create an initial population with a predefined population size. The population contains number of individuals (i.e., chromosomes).

In *GAs*, a possible solution to a problem is referred to as an individual, which is represented by a computational data structure called a chromosome. Chromosomes are strings of DNA and serves as a model of the whole organism. A chromosome consists of genes, blocks of DNA. Each gene encodes a particular protein. Each gene has its own position in the chromosome. This position is called locus. Complete set of genetic material (all chromosomes) is called genome. Particular set of genes in genome is called genotype. The genotype is with later development after birth base for the organism's phenotype, its physical and mental characteristics, such as eye color, intelligence etc. Algorithm is started with a set of solutions (represented by chromosomes) called population. Solutions from one population are taken and used to form a new population. This is motivated by a hope, that the new population will be better than the old one. Solutions which are selected to form new solutions (offspring) are selected according to their fitness - the more suitable they are the more chances they have to reproduce.

Each individual represents a solution for the problem under study. In our case, each solution is in fact a path between the start and end point in the search space.

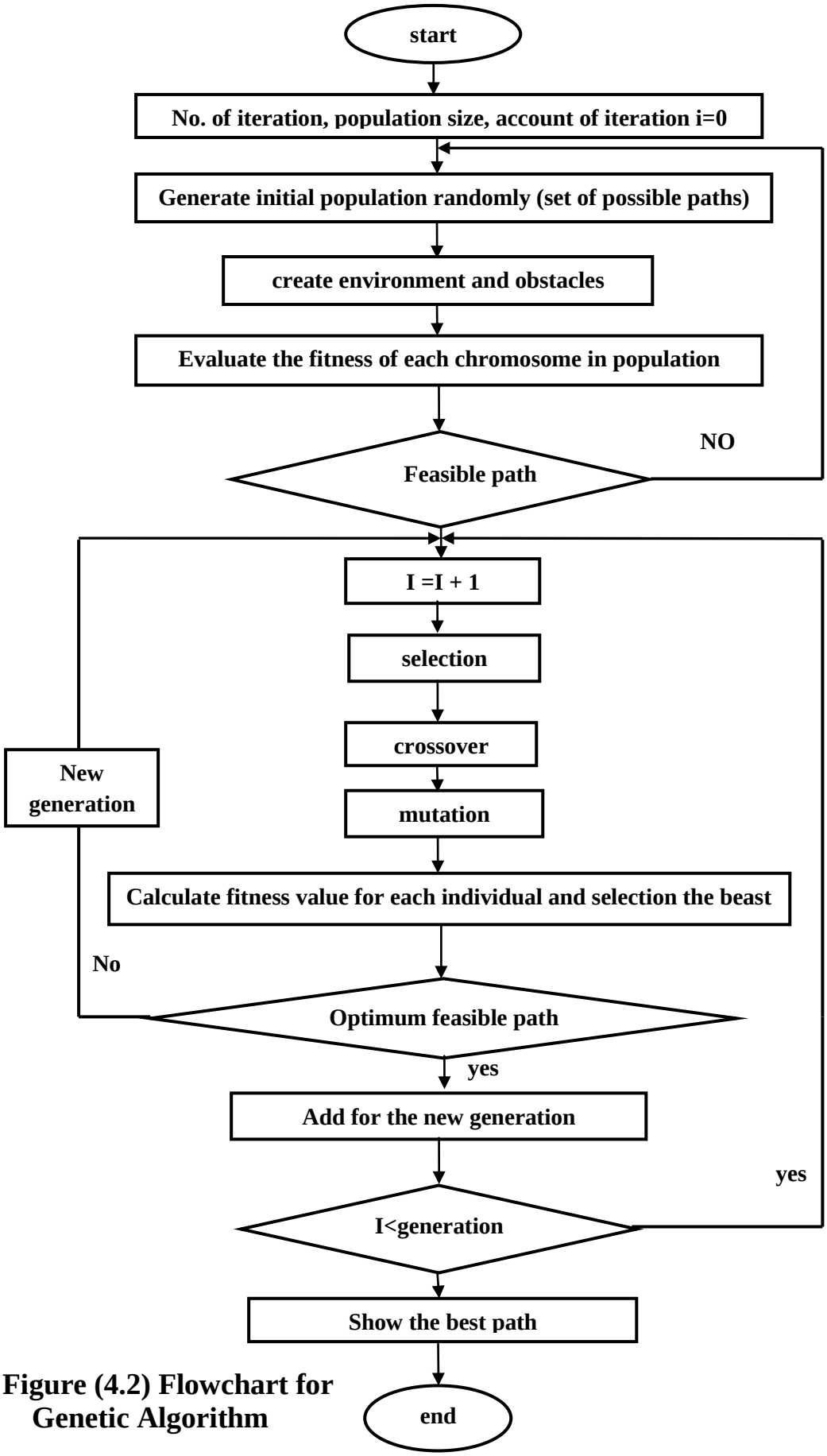

Figure (4.2) Flowchart for Genetic Algorithm

All individuals of the initial population are assumed to be generated randomly. This leads to generate large number of infeasible paths which intersect an obstacle, and infeasible paths should be avoided. If there are obstacles either in the vertical direction or horizontal direction, the mobile robot has to keep itself away from the obstacles. Initial population is stored in a single matrix. Each row corresponds to a particular solution. After generating the initial population, and to allow the robot to move between its current and final configurations without any collision within the surrounding environment, each individual must be checked whether it intersects with obstacle or not.

(ii) Fitness Function

The key component of the GA is fitness function which quantify the optimality of a solution (chromosome) so that a particular solution may be ranked against all the other solutions. The function depicts the closeness of a given 'solution' to desired result. The fitness function will lead the search towards the optimal solution. The optimal path is the shortest path between the starting and goal point. The fitness function is responsible on finding this path.

The length of the feasible path is compute as shown in Equation (4.1)

$$r_{(i)} = \sqrt{(x_{(i+1)} - x_{(i)})^2 + (y_{(i+1)} - y_{(i)})^2} \qquad \text{…..(4.1)}$$

The shortest path helps computing the total number of steps the robot need to take until reaching the end point. The objective function of the overall path can be expressed as shown in Equation (4.2)

$$r_{total} = \sum_{i=1}^{n} r_{(i)} \qquad \text{…..(4.2)}$$

Where: n is the number of points on the path from start point to goal point, $r_{(i)}$ is the distance between two points, $x_{(i)}$ and $y_{(i)}$ are robot's current horizontal and vertical positionsrespectively,$x_{(i+1)}$ and $y_{(i+1)}$ are robot's next horizontal and vertical positions.

The fitness function is the inverse of the total distance which is Euclidean distance. The Euclidean distance between starting and goal point is the length of the line segment connecting them. The fitness function used in this study is:

$$F = \frac{1}{r_{total}} \qquad \text{.....(4.3)}$$

Where *F:* is the fitness function .It is obvious that the best individual will have the maximum fitness value. At each generation (iteration), all the chromosomes will be updated by their fitness. A chromosome with good fitness has a much higher probability than other inferior chromosomes to appear in the next generation.

(iii) Environment

We used Genetic Algorithms to work space of (15×18) and (270) nodes to find an optimal path for a robot to move from start to end points.

Boundaries for obstacles area are formed by their actual boundaries plus a safety distance that is defined with consideration to the size of the robot. The obstacles are putting randomly but carefully placed such that they keep some distance from the starting point and the goal point to make sure that the robot has some space to move in the begging.

A potential path is formed by line segment which is connecting the points falling on of the working environment. The points are represented by their respective x and y coordinates. Each path is represented by two

chromosomes. The first chromosome is for *x*-coordinate and the second one is for *y*-coordinate.

(iv) Selection Process

Selection is the stage of a genetic algorithm in which individual genomes are chosen from a population for later breeding (recombination or crossover). There are several generic selection algorithms, such as tournament selection and fitness proportionate selection (also known as roulette-wheel selection). To selectively reproduce the population to determine the next generation we used elitism method which biased random selection procedure based on fitness.

(v) Crossover Operator

To better explore potential solutions Gas was employed a crossover operator, which mimics the reproduction process. Two individuals are mated by an exchange of these characteristics, and two child chromosomes are created. A randomly selected set of patterns from the parents are then exchanged to form two child chromosomes. The crossover techniques used here is single point crossover and the crossover. Two selected chromosomes are referred to as the parents. Children are generated by concatenating the first half of the first parent and second half of the second parent and vice versa. Thereby two off springs are generated. After performing crossover, the offspring produced forms the new generation. Genes from parents form in some way the whole new chromosome. The new created offspring can then be mutated.

(vi) Mutation

After a crossover is performed, mutation take place. This is to prevent falling all solutions in population into a local optimum of solved problem. Typically mutation will involve swapping two randomly selected bits in a chromosome. The next reproduction operation to be

performed is mutation where a particular gene in the chromosome gets changed. As in the crossover a random number is generated to determine the position where the mutation has to be performed.

(vii) Generation Algorithm

Commonly in the complex environment along with high density of obstructions the number of generated path is inefficient. Generation algorithm is used to increase the population and help to prevent the stagnating at local optima. Then the new generated population must be checked for infeasibility. If the number of generated path is still insufficient a new population is generated. This process is repeated over again until the desired number of feasible path is reached. So the proposed method does not use fixed population size but adaptive population size. Generated population formed in this way increase the efficiency of the proposed algorithm, and will not lose the overall genetic algorithm searching capabilities. In the next iteration, generation algorithm continues generate path instead of infeasible path. Genetic algorithm is terminated when the maximum number of iteration exceeds a certain limit, and also terminated when it does not find a path from the start point to the goal point.

4.6 Experimental Work

The implementation and applying of optimization path planning using program of genetic algorithm must be applied experimentally to provide guarantee for the robot motion, from the optimal path and pass through the waypoint and parameters values which contain angles for each robot joints. These values that obtained from experimental work will be the optimum parameters for this robot. In this study the experimental work will be applied on the Lab-Volt RoboCIM shown in Figure (4.3).

Figure (4.3) The Lab-Volt Servo Robot System Model 5250(RoboCIM5250)

The Lab-Volt Servo Robot System Model 5250(RoboCIM5250) automation robots are powerful, precision built, articulated arm, 5-axes of rotation plus a gripper. It is able to use all joints simultaneously to

perform a programmed move sequence. Robots are designed in every way to emulate industrial robots in their programming and operating features.

The robots feature advanced capabilities that distinguish them as high-precision, industrial quality systems, ideal for training in state-of-the-art manufacturing technology.

The Controlled Robot System, comes with the file transfer software to download and upload programs created. The robot software for the computer-controlled robot system, allows the robot to be directly controlled from the computer. This software provides a real-time 3D simulation of the robot and its immediate environment. Through an intuitive dragand- drop interface, users can directly control the position and movement of the robotic arm.

The Lab-Volt RoboCIM software is used to simulate and control the operation of the Servo Robot and external devices, and create programs.

4.6.1 Coordinates of Robot Motion

The position of the RoboCIM software, displays articular and cartesian coordinates representing the current position of the robot. The five values ("Base, Shoulder, Elbow, W. Pitch, and W. Roll") represent the articular coordinates, while the other five values ("X, Y, Z, Pitch, and Roll") represent the end-effector coordinates.

To achieve optimization path we must enter the coordinate of start and goal points. There are two types of coordinate systems used for motion: the cartesian coordinates and the articular coordinates.

• The **Articular** coordinates system: prescribes motion on each of the eight joints, i.e. the five articulations on the robot (base, shoulder, elbow, wrist pitch, and wrist roll). When using the articular coordinates system to move the robot, we do not control the trajectory between the initial and

final positions. The movement between two points will not be linear. In other words, it will not follow a straight line between the two points. Consequently, it is not recommended to use the articular coordinates system when an accurate displacement between points is needed.

• The **Cartesian** coordinates system: prescribes motion on the end effector of the robot. When using the Cartesian coordinates system to move the robot, the trajectory between the initial and final positions will be linear. In other words, it will follow a straight line between the two points. Thus, this type of coordinate system is recommended when you need to have accurate displacement between points.

4.6.2 Experimental Procedure

• RoboCIM workspace is created and adjusted the dimension of work space and change robot position Figure (4.4) and Figure (4.5).

• The start and goal points are determined and the free points in the environment of robot are defined, Figure (4.6).

• An obstacle is added to the workspace by giving the limitations of these obstacles.

• The program of robot motion using is created and run either in the text programming mode or the icon programming mode.

Icon program: allows you to create and run simple task programs, with the aid of icons and graphical tools (no typewriting required).

Text program: allows you to create and run simple and complex task programs, by typewriting all necessary commands Figure (4.7).

• Then the real system is connected.

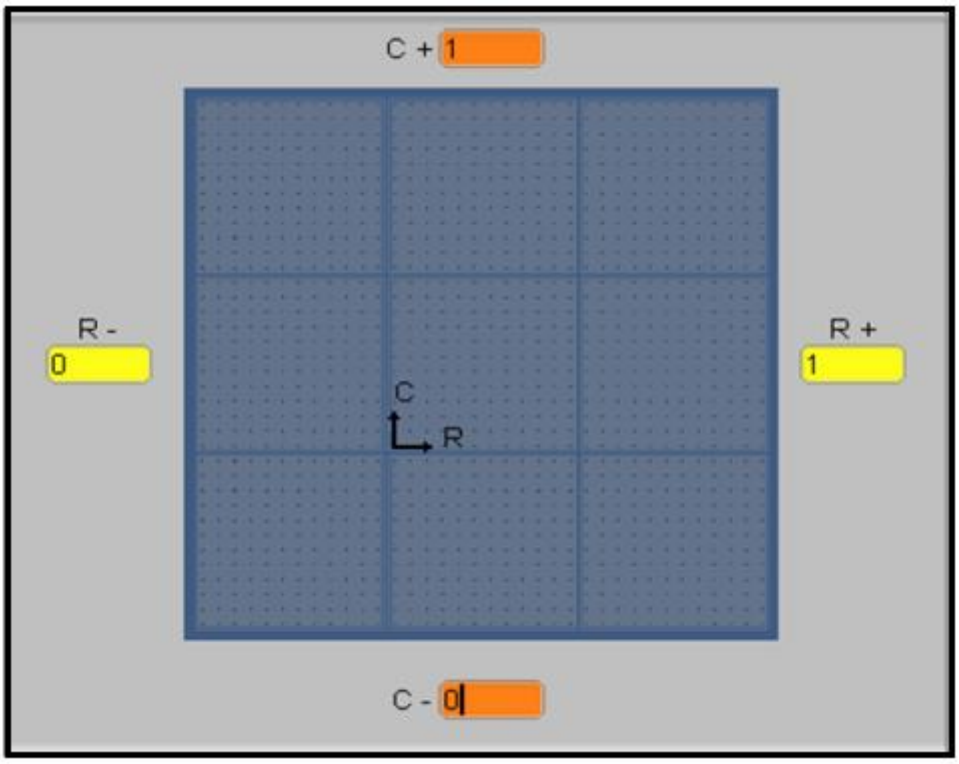

Figure (4.4) Setting the Work Surfaces of Robot.

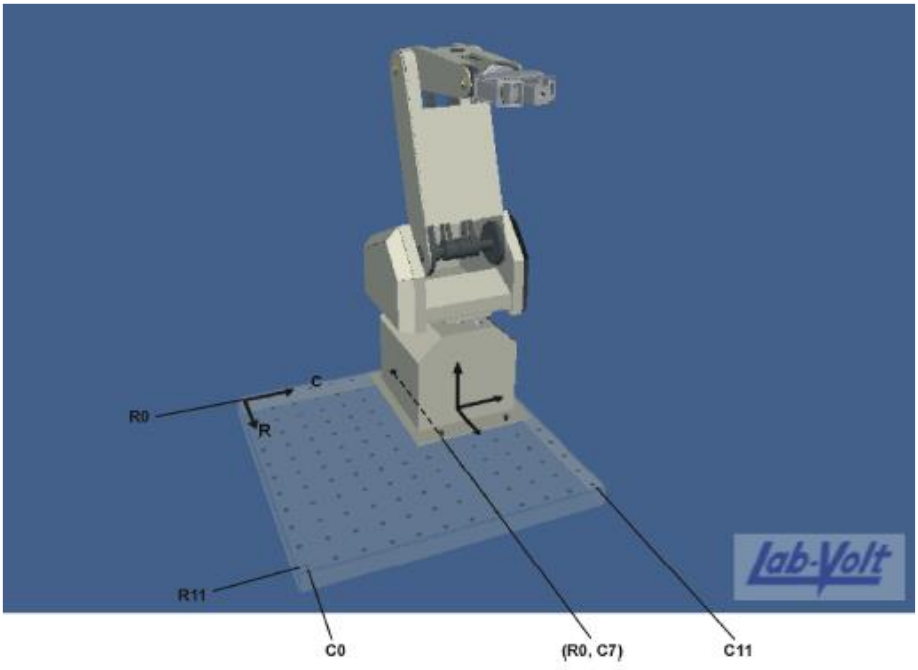

Figure (4.5) Change Robot Position in the Work Space.

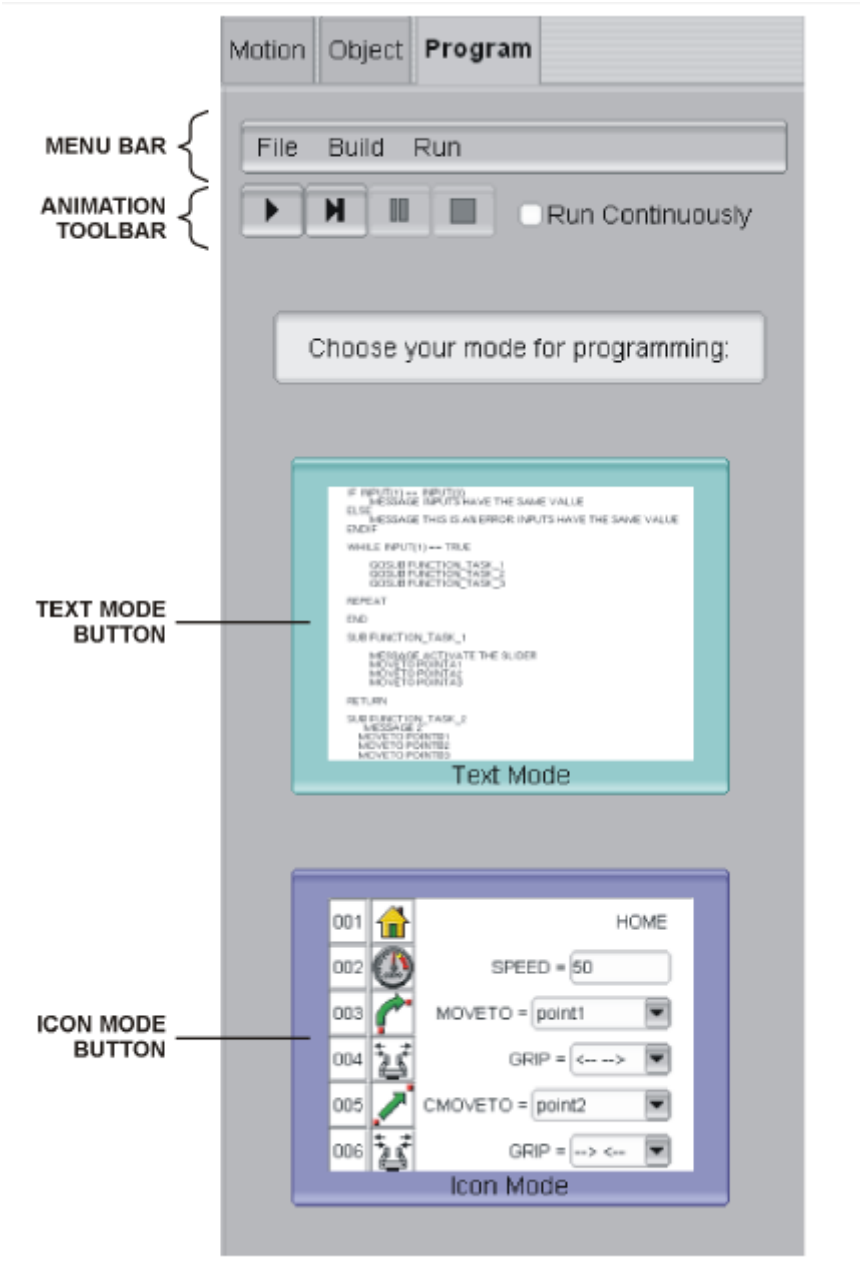

Figure (4.6) Preface Program of Robot

Figure (4.7) The RoboCIM5250 Connected With Component

CHAPTER FIVE

RESULTS AND DISCUSSIONS

5.1 Introduction

The results of Genetic Algorithm program (GA) are presented to find the optimal path along the obstacle-free directions. To illustrate their wide applicability and their effectiveness, the algorithm results are implemented practically by using lab volt RoboCIM in the unit of robotics in the department of control and systems - University of Technology software for solving the path problem through the computer simulation for working environment to obtain the optimal parameters at optimal positions.

The implementation of genetic algorithm (GA) to solve optimization path of robot problem is demonstrated. The working environment has been proposed to test the performance of this algorithm to find the optimal or near optimal path. In all cases, an optimal path is formed by line segment which is connecting the start and goal points of the working environment.

The performance of the genetic algorithm (GA) has been tested by applying genetic algorithm (GA) to the working environment presented in Figure (4.2). This result was ascertained by using it experimentally. So the results are categorized into program results and experimental results.

5.2 Genetic Algorithm Program Results and Discussions

In this section, the simulation results of optimization using Genetic Algorithm (*GA*) is presented to find the optimal path along the obstacle-free directions. The performance of the Genetic Algorithm (*GA)* has been tested by applying Genetic Algorithm (*GA)* to the working environment presented Figure (4.2)**.**For the proposed algorithm the simulation parameters are: population size =100, multi generation for various environment. The programs are written in MATLAB 2013a.

In this study we propose two different environments with various obstacles locations. They include moderate environment by change locations and shapes of obstacles randomly.

Genetic Algorithm (GA) will be run with various generations for each environment. The objective is to investigate the behavior of Genetic Algorithm (GA) in each case. This will also help in showing that Genetic Algorithm (GA) will converge to the optimal solution (i.e., optimal path) in each run.

The first environment: Table (5-1) and figures (5.1) to (5.6) show the computed results using Genetic Algorithm (GA) with various generations. The best distance value was achieved after each run and the generation number where this value was found. The program results of the Genetic Algorithm (GA) show that shortest generated path (distance) with the length of (24.21) at generation (60) as shown in Figure (5.6). The units of both direction in (cm).

Figure (5.7) shows the increasing in the number of generation gives the shortest path with the same number of population size and gives less distance of path.

Table (5-1) Program Results For The First Working Environment Using (GA) With Population Size 100.

Exp #	Generation No.	Distance
1	20	33.49
2	25	30.46
3	35	24.44
4	40	24.29
5	50	24.22
6	60	24.21

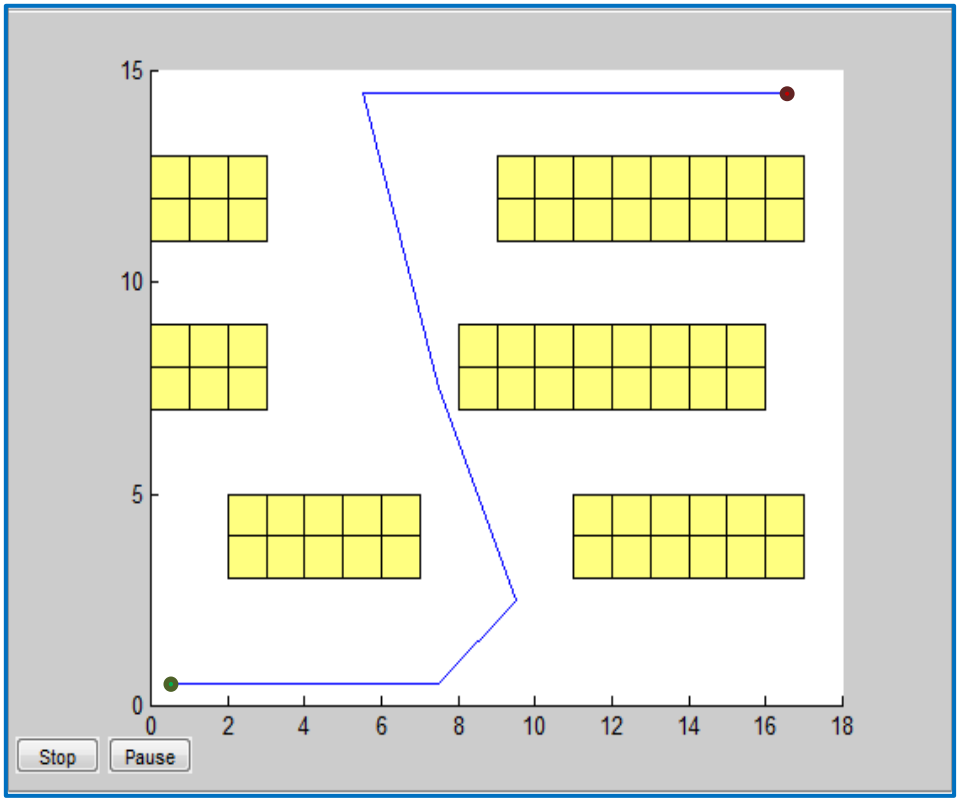

Figure (5.1) Feasible Path For The First Working Environment Using GA (20 Iterations)

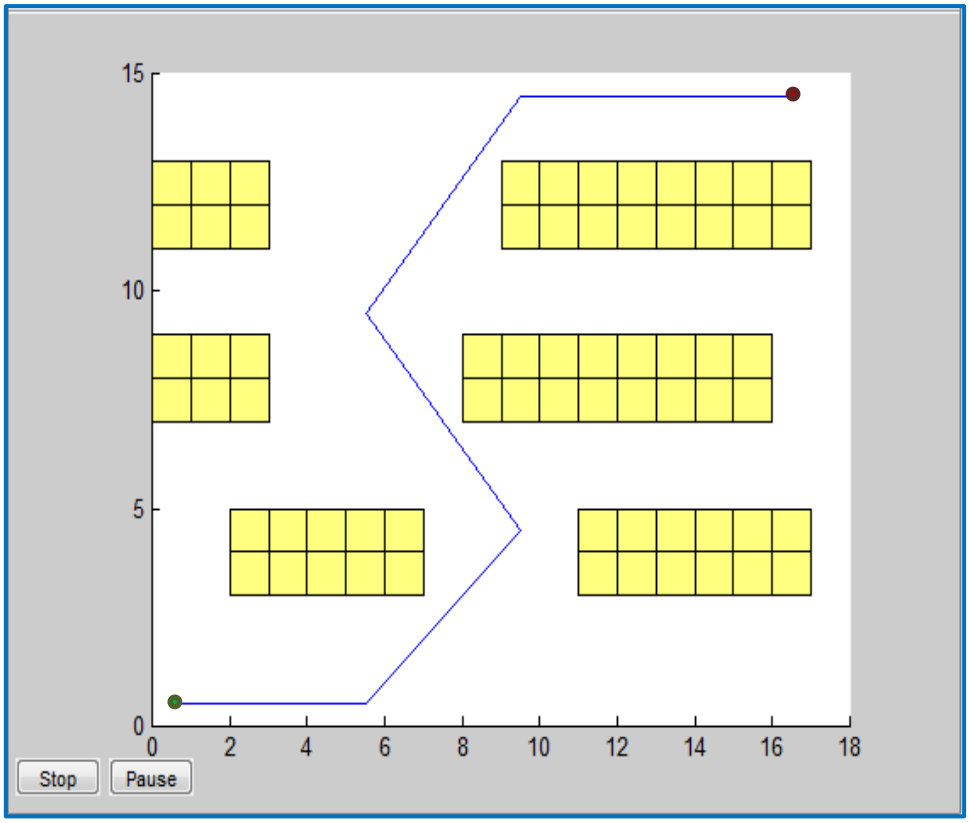

Figure (5.2) Feasible Path For The First Working Environment Using GA(25 Iterations)

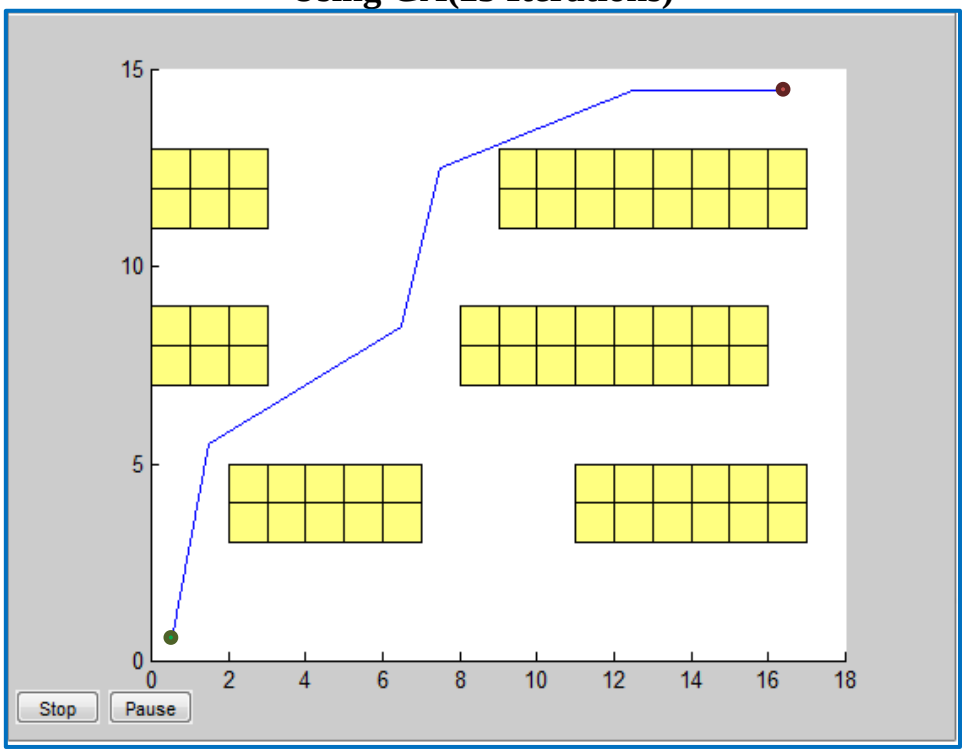

Figure (5.3) Feasible Path For The First Working Environment Using GA(35 Iterations)

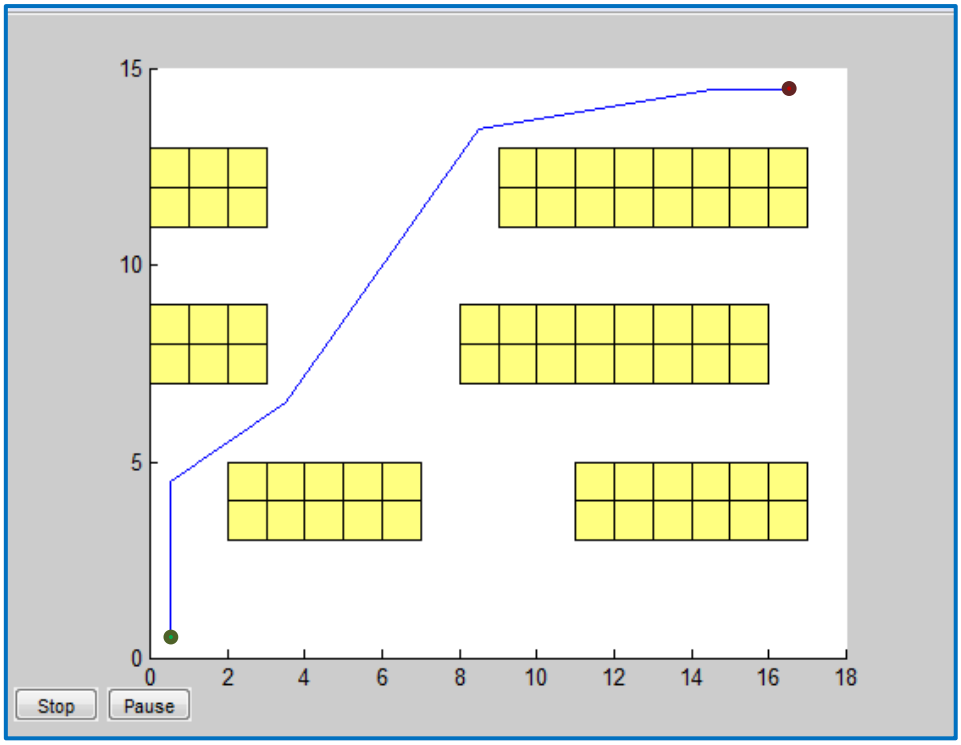

Figure (5.4) Feasible Path For The First Working Environment Using GA(40 Iterations)

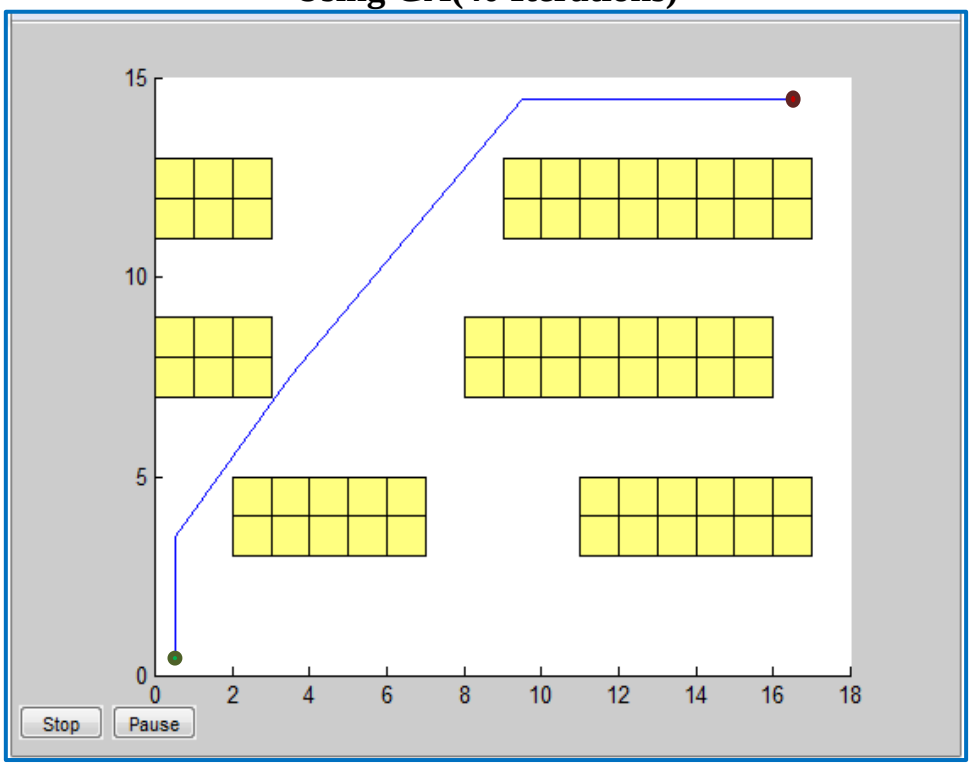

Figure (5.5) Feasible Path For The First Working Environment Using GA(50 Iterations)

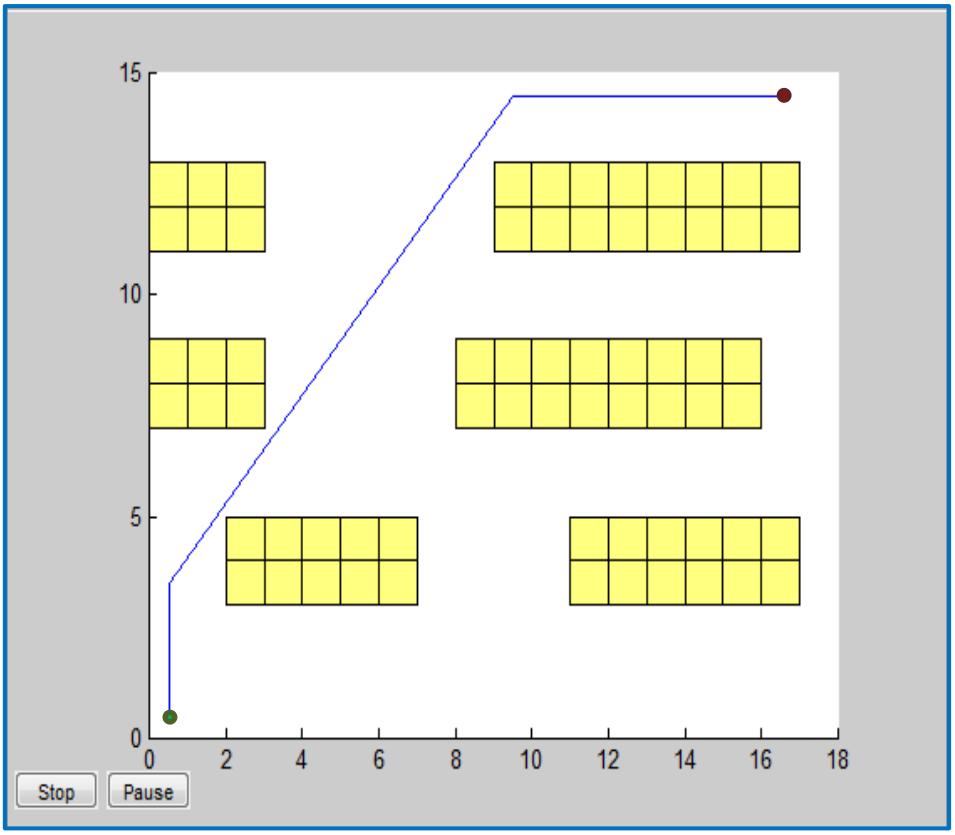

Figure (5.6) Feasible Path For The First Working Environment Using GA(60 Iterations)

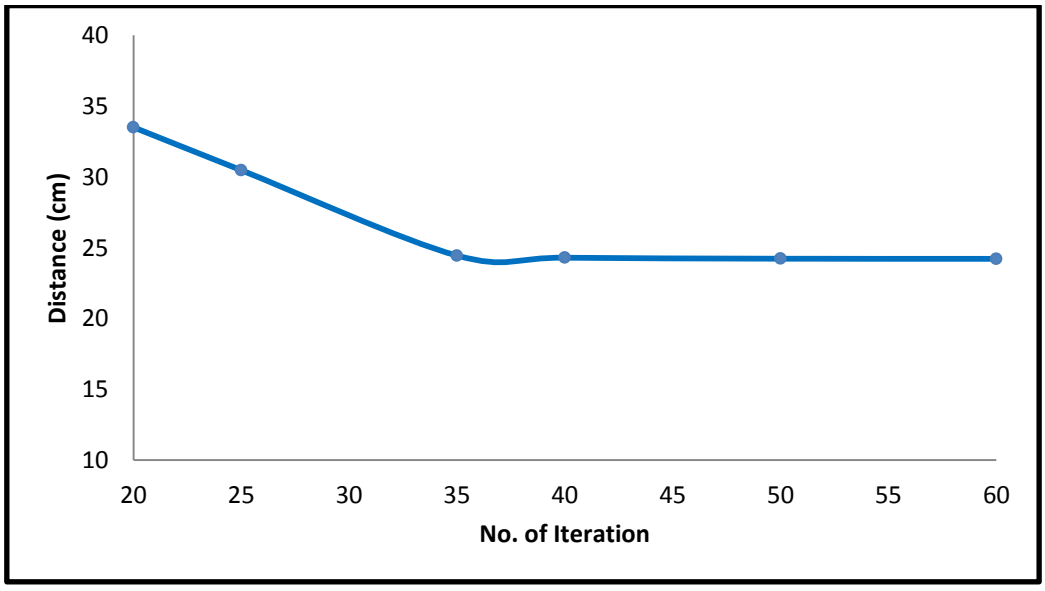

Figure (5.7) Convergence Process For GA With The Environment

The second environment: The position, shapes and number of obstacles are shown in Figures(5.8) to (5.13). Table (5-2), shows the discovered paths using Genetic Algorithm (GA) with the moderate environment. The program results show that shortest generated path of the second environment is (22.52) with generation (400), see Figure (5.13). It was found the program can be successful in both simple or complex environment but in complex environment the number of generation will be increased to obtain the optimal path with the same number of population size for each case.

Table (5-2) Program Results For The Moderate Working Environment Using GA With Population Size 100.

Exp #	Generation No.	Distance
1	25	33.17
2	100	25.24
3	150	24.28
4	200	23.25
5	300	22.65
6	400	22.52

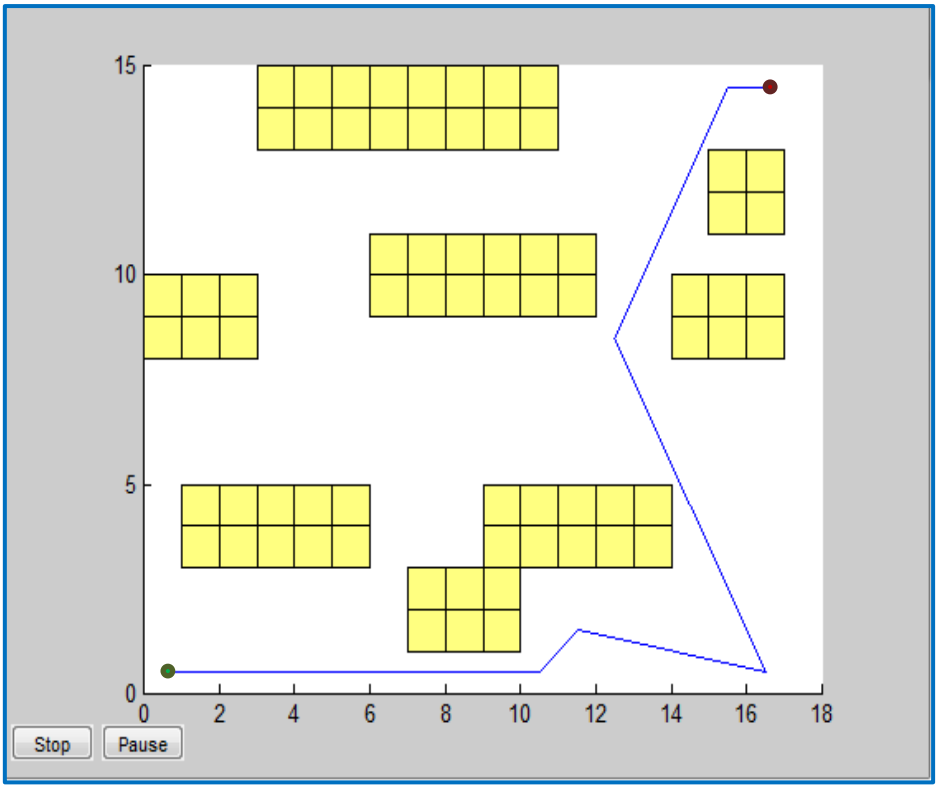

Figure (5.8) Feasible Path For The Moderate Working Environment Using GA(25 Iterations)

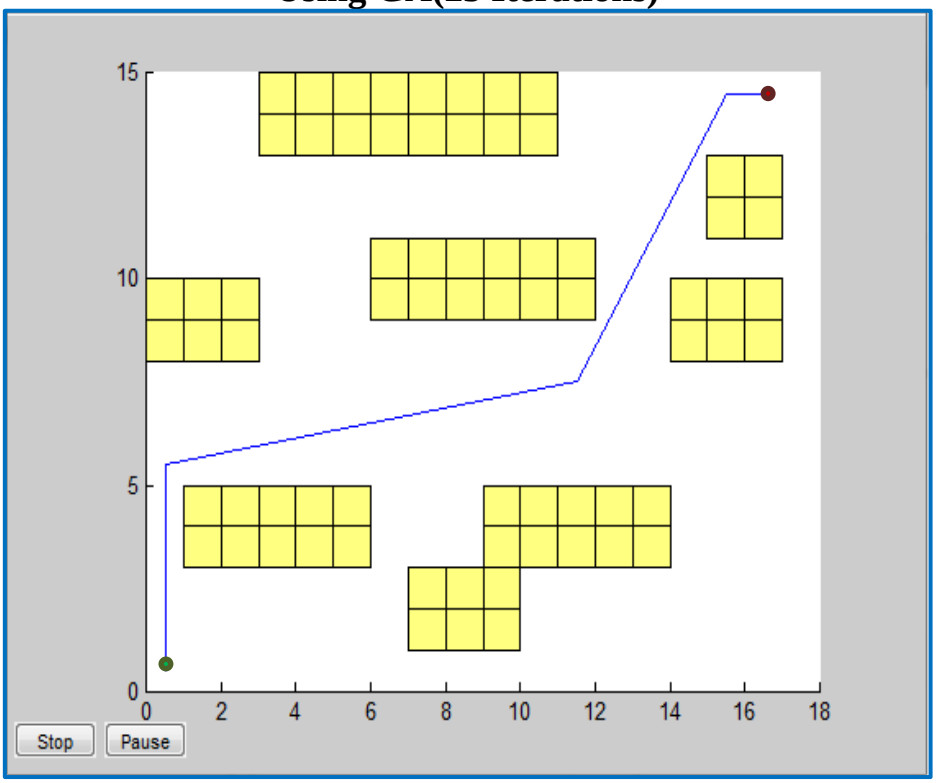

Figure (5.9) Feasible Path For The Moderate Working Environment Using GA(20 Iterations)

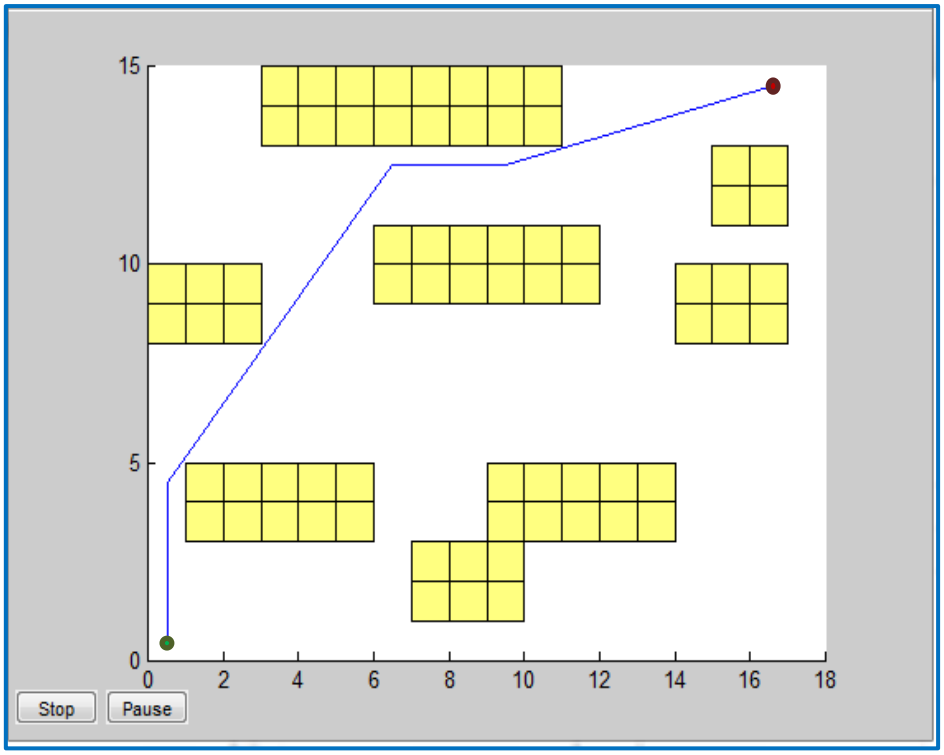

Figure (5.10) Feasible Path For The Moderate Working Environment Using GA(100 Iterations)

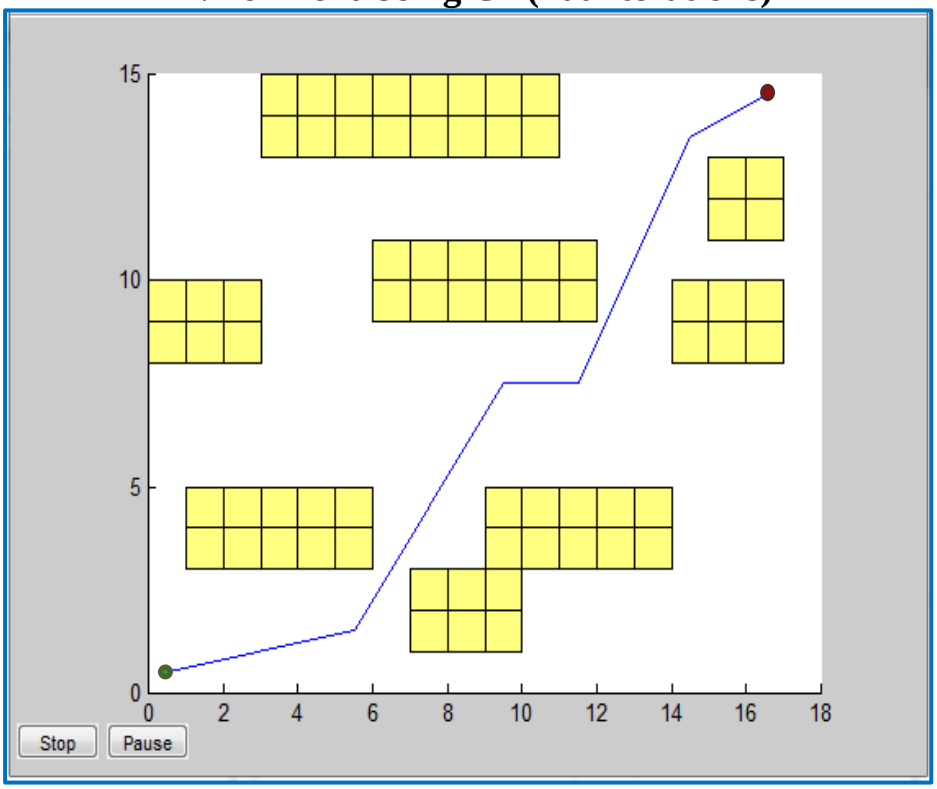

Figure (5.11) Feasible Path For The Moderate Working Environment Using GA(150 Iterations)

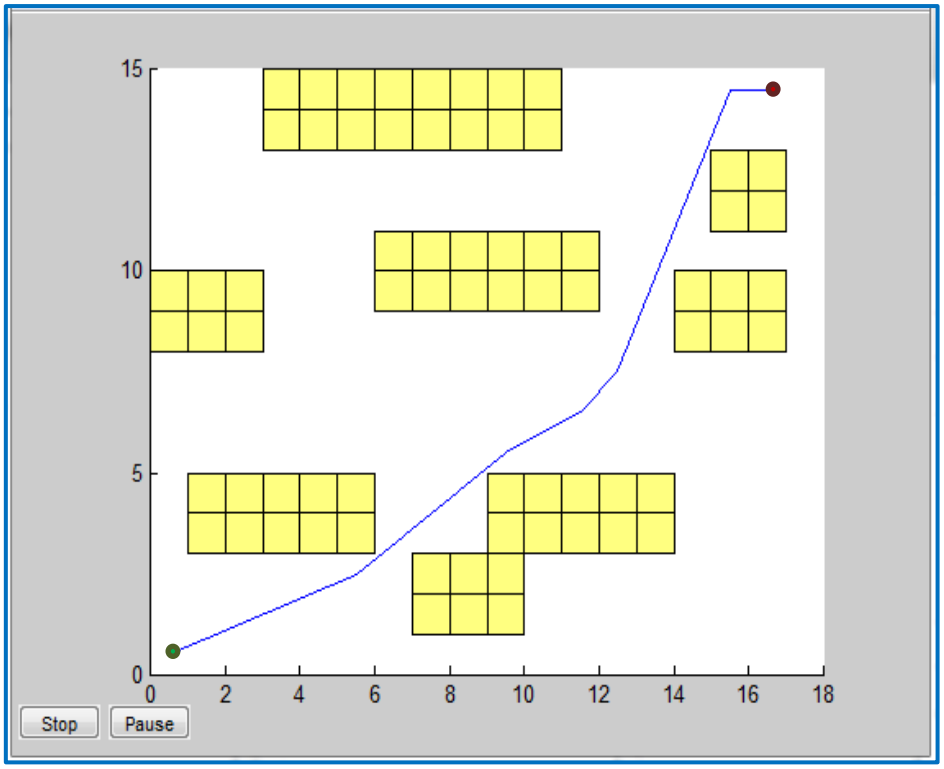

Figure (5.12) Feasible Path For The Moderate Working Environment Using GA(300 Iterations)

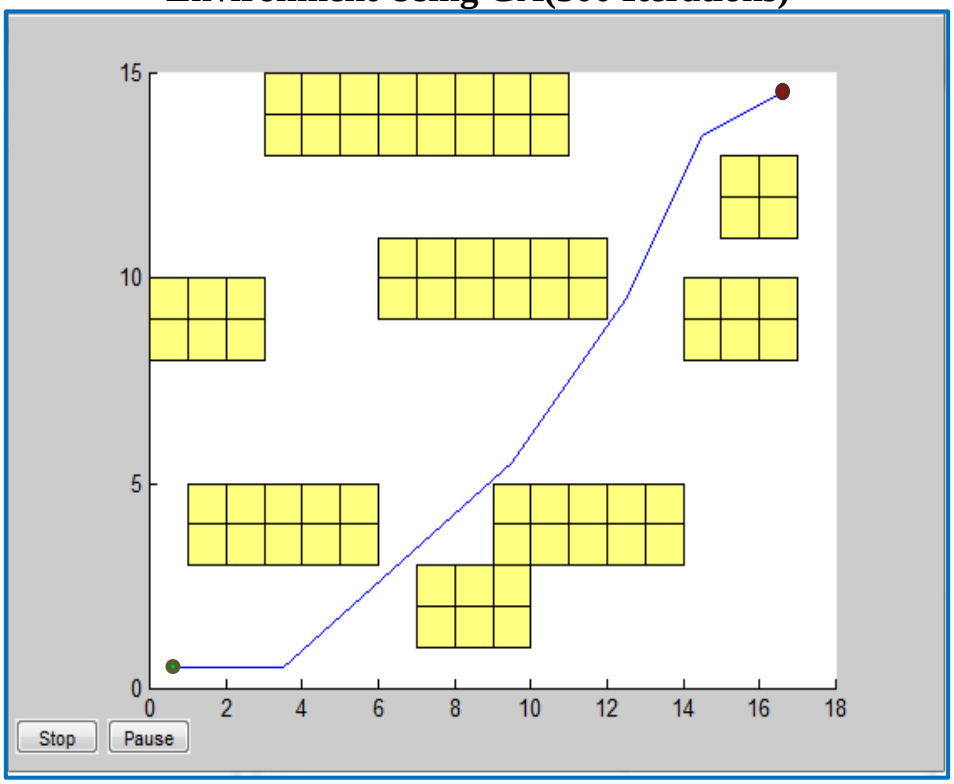

Figure (5.13) Feasible Path For The Moderate Working Environment Using GA(400 Iterations)

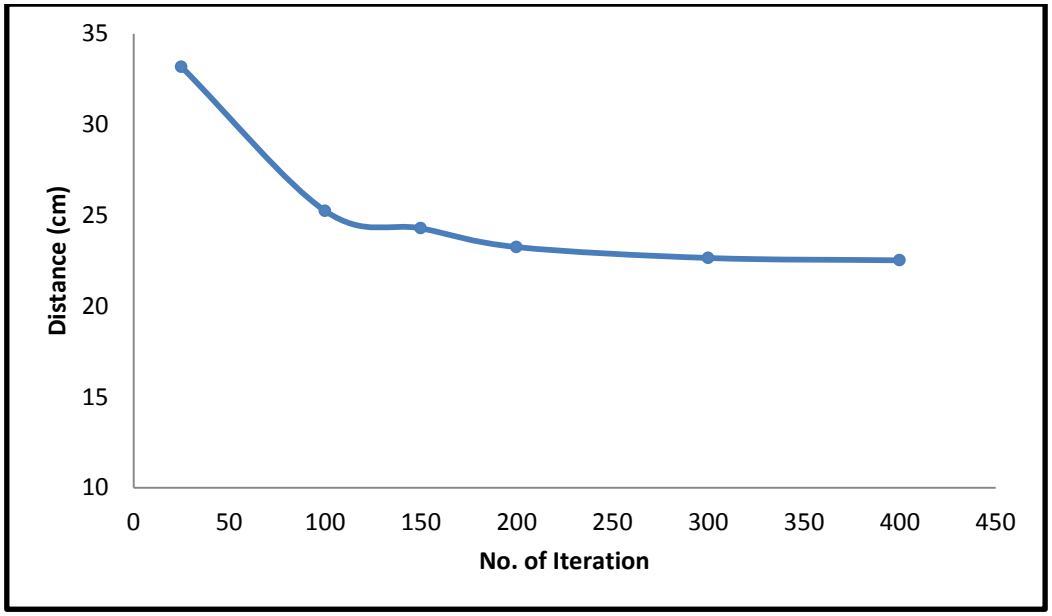

Figure (5.14) Convergence Process For GA With The Moderate Environment

5.3 Experimental Results and Discussions

After the optimal results are obtained and entered the results on the robot software and simulation runs then connected practically. By applying the experimental procedure; the optimal parameters of robot are presented.

Each point on the path has cartesian and articular coordinates. The points describe the position of the robot. The type of coordinates system used for motion: cartesian coordinates or articular coordinates depend on the selected type of coordinates system, either the cartesian coordinates or articular coordinates will be displayed. Since the coordinates displayed are dependent upon each other (that is, the position and orientation of the end-effector depend on the articulation coordinates).

For the robot, three different kinds of axes can be shown. The first one is the robot base axes, displayed at the bottom of the robot and representing the Cartesian coordinates origin (X = 0, Y = 0, Z = 0). These axes are always shown. The second type is the robot articulation axes, displayed at

each articulation of the robot. The last type of axes is the robot end-effector axes, displayed at the extremity of the robot.

Each optimal position has five values ("Base, Shoulder, Elbow, W. Pitch, and W. Roll") that represent the Articular coordinates, and five values ("X, Y, Z, Pitch, and Roll") represent the end-effector coordinates. The optimization results of coordinates for robot in each position points are shown in tables (5.3) to (5.6), figures (5.15) and (5.15) show the end effector of robot at each point of the optimal path (yellow point).

Table (5.3) The Optimization Values of Cartesian Coordinates For Robot At Each Point. (All Unites In mm)

Point	x-value	y-value	z-value
1	1.5	-280	47.5
2	41.5	-225	47.5
3	146.5	-170	47.5
4	256.5	105	47.5

Table (5.4) The Optimization Values of Articular Coordinates For Robot At Each Point. (All Unites In Degrees)

Point	Base	Shoulder	Elbow	Wrist Pitch	Wrist Roll
1	-89.69	6.63	-117.62	110.98	0.31
2	-79.55	1.98	-128.32	126.34	10.45
3	-49.25	1.45	-129.2	127.75	40.75
4	22.26	6.45	-118.23	111.79	112.26


1


2

Figure (5.15):The End- effector of RoboCIM5250 at Each Point In The First Workspace.

Table (5-5) The Optimization Values of Cartesian Coordinates for Robot at Each Point in the Second Workspace. (all unites in mm)

Point	x-value	y-value	z-value
1	-198	-409.5	47.5
2	-106.5	-409.5	47.5
3	76	-242	47.5
4	183	-135.5	47.5
5	229	-13	47.5
6	290	17.5	47.5

Table (5-6) The optimization values of articular coordinates for robot at each point in the second workspace.(all unites in degrees)

Point	Base	Shoulder	Elbow	Wrist Pitch	Wrist Roll
1	-115.8	5.89	-71.86	65.97	334.2
2	-104.58	7.66	-81.77	74.12	345.42
3	-72.57	4.6	-123.24	118.64	17.43
4	-36.52	1.85	-128.54	126.69	53.48
5	-3.25	2.05	-128.21	126.16	86.75
6	3.45	7.26	-115.3	108.05	93.45

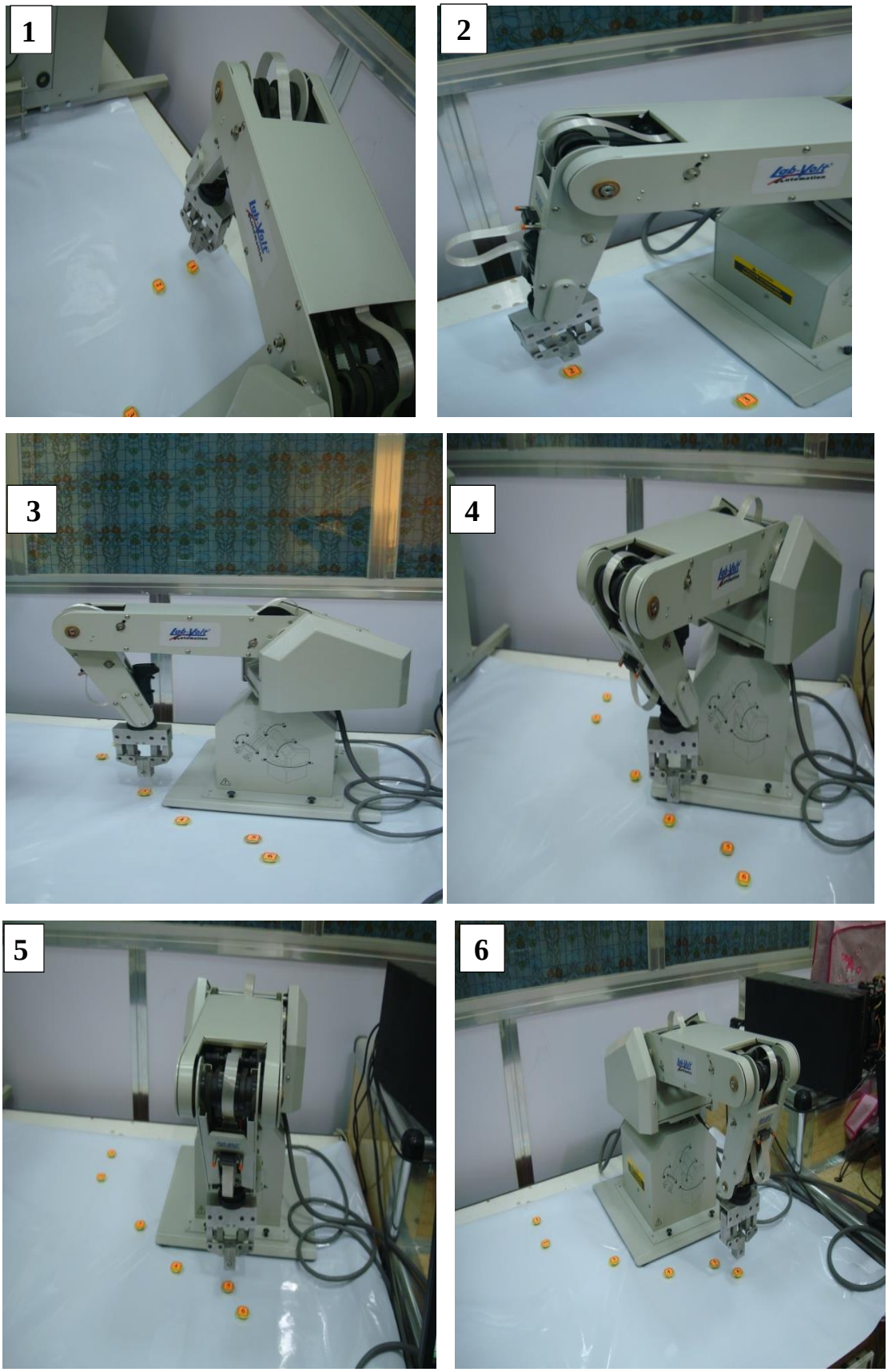

Figure (5.16) The End- effector of RoboCIM5250 at Each Point in the Second Workspace

5.4 Motion and Forces Analyses for Grasper

Figure (5.17) shows the relationship between the outer length of jaw (JL1) with backward horizontal motion for different jaw opening width (Δb). It decreases with increased of the length of (JL1) as well as increased jaw opening. We found from program results that best value of counting jaw opening equals 18mm. That is when the length JL1 equals 31.272 mm. This value will be best when the whole size to grasper is decreased which gives a good motion in workspace.

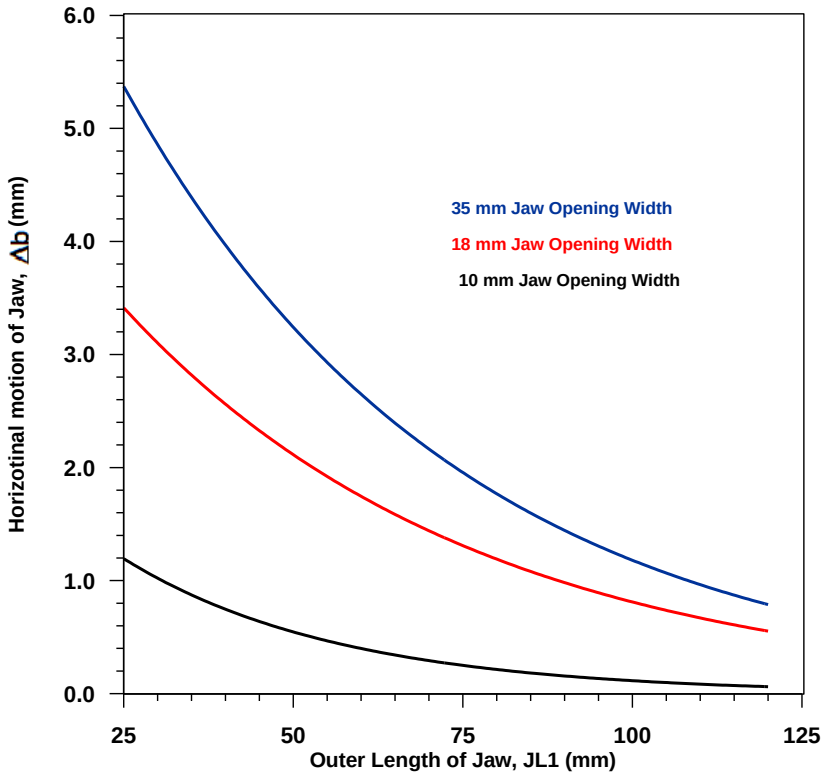

Figure (5.17) The Outer Length of Jaw with Backward Horizontal Motion For Different Jaw Opening Width

CHAPTRE SIX

CONCLUSIONS AND RECOMMENDATIONS

6.1 Introduction

This work includes a theoretical analysis to obtain the optimization path planning using genetic algorithm method and experimental work for laparoscope with seven degrees of freedom. It also includes studying of the parallel jaws tool.

6.2 Conclusions

The conclusions that are extracted from the present study are as following:

1. In this study we presented the idea of using Genetic Algorithm (GA) approach to solve the optimization path planning problem in environment with variable number of generation. This idea shows that the proposed approach is effective and efficient in handling different types of tasks environments.
2. Genetic Algorithm (GA) will determine the way point accurately. It can help to choose the near points or the optimal points and ignore unfeasible points. This technique of Genetic Algorithm (GA) gives the unique optimal path.
3. We proposed a simplified fitness function which utilizes the path length.
4. We explored the performance of the evolutionary process with various number of generations.
5. We increased the number of generation to obtain a shortest and smoother path that is safer in both types of environments.
6. With increasing the complexity of the environment the number of generation must be increased with fixed population size.

7. The parallel play of grasper jaws has good properties like the small size relative to workspace according to this. They can be bent in workspace.

5.2 Recommendations for Future Work

The recommendations for future work on the optimization are listed below:

1. It is possible to have an optimization of DOF (degree of freedom) for the end part of manipulator according to surgical operations.
2. Other optimization methods can be selected such as simulated annealing, harmony, particle swarm optimization and ant colony system (ACS) to find the optimal path.
3. Extend the optimization study to include other components of surgical system.
4. Apply the output of the program on surgical robot instead of industrial robot to obtain optimal parameter values.
5. Study other types of the Grasper.

Appendix B

B-1 Inverse kinematic analysis

To determine the value of angles and the distance

$$ {}^{0}_{2}T^{-1}\,{}^{0}_{7}T = {}^{2}_{7}T $$

$$ \begin{bmatrix} c_1c_2 & s_1c_2 & -s_2 & 0 \\ -c_1s_2 & -s_1s_2 & -c_2 & 0 \\ -s_1 & c_1 & 0 & -l_1 \\ 0 & 0 & 0 & 1 \end{bmatrix} \begin{bmatrix} r''_{11} & r''_{21} & r''_{13} & p''_x \\ r''_{21} & r''_{22} & r''_{23} & p''_y \\ r''_{31} & r''_{32} & r''_{33} & p''_z \\ 0 & 0 & 0 & 1 \end{bmatrix} = \begin{bmatrix} r'_{11} & r'_{21} & r'_{13} & p'_x \\ r'_{21} & r'_{22} & r'_{23} & p'_y \\ r'_{31} & r'_{32} & r'_{33} & p'_z \\ 0 & 0 & 0 & 1 \end{bmatrix} $$

To find θ_1 from left ($ {}^{1}_{3}R $, $ {}^{2}_{4}C $) and right ($ {}^{3}_{3}R $, $ {}^{3}_{3}C $)

Where $ {}^{b}_{a}R $

(R) is row (a) is number of row (b) name of matrix as assume of (C) is column.

$$ -s_1\,p_x + c_1p_y - L_1 = 0 $$

$$ -s_1\,p_x + c_1p_y = L_1 $$

$$ \therefore \theta_1 = \text{A tan2}\,(-p_x, p_y) \pm (\text{A tan2}\,(\sqrt{p_x^2 + p_y^2 - L_1^2}, L_1) $$

To find d_4 from ($ {}^{1}_{1}R $, $ {}^{2}_{4}C $) and ($ {}^{3}_{1}R $, $ {}^{3}_{4}C $) and ($ {}^{1}_{2}R $, $ {}^{2}_{4}C $) ($ {}^{3}_{2}R $, $ {}^{3}_{4}C $)

$$ c_1c_2\,p_x + s_1c_2p_y - s_2\,p_z = -s_3\,(L_3 + L_2 - d_4) $$

$$ -c_1s_2\,p_x - s_1s_2p_y - c_2\,p_z = -c_3(L_3 + L_2 - d_4) $$

By

$$ c_1^2c_2^2p_x^2 + 2\,c_1\,s_1\,p_x\,p_yc_2^2 - 2\,c_1\,c_2s_2\,p_xp_z = s_1^2c_2^2 $$

$$ p_y^2 + s_2^2\,p_z^2 - 2\,s_1\,s_2\,p_y\,s_2\,p_z = s_3^2(L_3 + L_2 - d_4)^2 \ldots.(1) $$

$$ c_1^2\,s_2^2\,p_x^2 + 2\,c_1s_1\,p_x\,p_y\,s_2^2 + 2\,c_1s_2c_2\,p_xp_z + s_1^2\,s_2^2\,p_y^2 + c_2^2\,p_z^2 + $$

$$ 2\,s_1s_2\,c_2\,p_y\,p_z = c_3^2(L_3 + L_2 - d_4)^2 \ldots. (2) $$

$$ d_4 = [L_3 + L_2 - (\,c_1^{\,2}\,p_x^{\,2} + 2c_1p_xp_y\,s_1 + s_1^{\,2}\,p_y^{\,2} + p_z^{\,2}]^{1/2} $$

Now; for find the value of θ_3:

$$ {}^{2}_{3}T^{-1} = \begin{bmatrix} c_3 & -s_3 & 0 & 0 \\ -s_3 & -c_3 & 0 & 0 \\ 0 & 0 & -1 & 0 \\ 0 & 0 & 0 & 1 \end{bmatrix} $$

$$ {}^{0}_{3}T^{-1} = {}^{0}_{2}T^{-1}\,{}^{2}_{3}T^{-1} $$

$$ {}^{0}_{3}T^{-1} = \begin{bmatrix} c_1c_2 & s_1c_2 & -s_2 & 0 \\ -c_1s_2 & -s_1s_2 & -c_2 & 0 \\ -s_1 & c_1 & 0 & -L_1 \\ 0 & 0 & 0 & 1 \end{bmatrix} \begin{bmatrix} c_3 & -s_3 & 0 & 0 \\ -s_3 & -c_3 & 0 & 0 \\ 0 & 0 & -1 & 0 \\ 0 & 0 & 0 & 1 \end{bmatrix} $$

$$ {}^{0}_{3}T^{-1} = \begin{bmatrix} c_1c_{23} & s_{13}c_2 & -s_2 & 0 \\ -c_{13}s_2 & -s_{13}s_2 & -c_2 & 0 \\ -s_{13} & c_{13} & 0 & -L_1 \\ 0 & 0 & 0 & 1 \end{bmatrix} $$

$$ {}^{0}_{3}T^{-1}\,{}^{0}_{7}T = {}^{3}_{7}T $$

$$ \begin{bmatrix} c_1c_{23} & s_{13}c_2 & -s_2 & 0 \\ -c_{13}s_2 & -s_{13}s_2 & -c_2 & 0 \\ -s_{13} & c_{13} & 0 & -L_1 \\ 0 & 0 & 0 & 1 \end{bmatrix} \begin{bmatrix} r_{11} & r_{12} & r_{13} & p_x \\ r_{21} & r_{22} & r_{23} & p_y \\ r_{31} & r_{32} & r_{33} & p_z \\ 0 & 0 & 0 & 1 \end{bmatrix} $$

$$ = \begin{bmatrix} r''_{11} & r''_{21} & r''_{13} & p''_x \\ r''_{21} & r''_{22} & r''_{23} & p''_y \\ r''_{31} & r''_{32} & r''_{33} & p''_z \\ 0 & 0 & 0 & 1 \end{bmatrix} $$

Now, take from the above matrix (${}^{1}_{3}R$, ${}^{2}_{4}C$) and (${}^{3}_{3}R$, ${}^{3}_{4}C$)

$-s_{13}p_x - c_{13}p_y - L_1 = 0$

$-s_{13}p_x - c_{13}p_y = L_1$

$\therefore \theta_{13}$ = A tan2 ($-p_x$, $-p_y$) $\pm$ (A tan2 ($\sqrt{p_x^2 + p_y^2 - L_1^2}$, L_1)

$\theta_3 = \theta_{13} - \theta_1$

Now, take from the above matrix:

(${}^{1}_{2}R$, ${}^{2}_{4}C$) and (${}^{3}_{2}R$, ${}^{3}_{4}C$)

$-s_2c_{13}p_x + s_2s_{13}p_y + c_2p_z = L_3 + L_2 - d_4$

$s_2(-c_{13}p_x + s_{13}p_y) + c_2p_z = L_3 + L_2 - d_4$

Assume A= $-c_{13}p_x + s_{13}p_y$; B = p_z ; C = $L_3 + L_2 - d_4$

$$\therefore s_2\,A + c_2\,B = C$$

θ_2 = A tan2 (A, B) $\pm$ (A tan2 ($\sqrt{A^2 + B^2 - C^2}$, C)

Now; take from the above matrix

From (${}^{1}_{2}R$, ${}^{2}_{3}C$) and (${}^{3}_{2}R$, ${}^{3}_{3}C$)

$-s_2c_{13}r_{13} + s_2s_{13}r_{23} + c_2r_{33} = -c_6$

Assume now; A= $-c_6$

$s_6 = \pm\sqrt{1-A^2}$

θ_6 = A tan2 ($\pm\sqrt{1-{c_6}^2}$, $-c_6$)

Same step

From (${}^1_1R$,${}^2_3C$) and (${}^3_1R$,${}^3_3C$)

$c_1c_{23}r_{13} - c_2s_{13}r_{23} + s_2r_{33} = -c_5s_6$

$$\therefore c_5 = \frac{-c_1c_{23}r_{13} + c_2s_{13}r_{23} + s_2s_{33}}{s_6}$$

Assume now; $c_5 = B$

θ_5 = A tan2 ($\sqrt{1-{c_5}^2}$, c_5)

Same step

From (${}^1_2R$,${}^2_2C$) and (${}^3_2R$,${}^3_2C$)

$-s_2c_{13}r_{12} + s_2s_{13}r_{22} + c_2r_{32} = s_6s_7$

$$s_7 = \frac{-s_2c_{13}r_{12} + s_2s_{13}r_{22} + c_2r_{32}}{s_6} = C$$

$c_7 = \sqrt{1-C^2}$

θ_7 = A tan2 ($\sqrt{1-{c_7}^2}$, c_7)

Appendix (C)

C-1 Piezoelectric Bimorph Grasper For Use In Surgical Applications

The word ‘piezoelectric’ is made up of two parts: ‘piezo’, which is derived from the Greek word for pressure, and ‘electric’ from electricity. Thus, the piezoelectric effect pertains to the coupling between pressure and electric charge/field. This phenomenon is generally referred to as ‘the direct piezoelectric effect’. Conversely, the application of an electric charge/field to the same material will result in a change of the physical dimensions, i.e. mechanical strain. This phenomenon is generally known as ‘the converse piezoelectric effect’. Several ceramic materials such as lead-zirconate-titanate (PZT), lead-titanate ($PbTiO_2$), lead-zirconate ($PbZrO_3$), and barium-titanate ($BaTiO_3$) have been known to exhibit a piezoelectric effect. In addition, the piezoelectric effect is found in a few polymers such as polyvinylidene fluoride (PVDF).

Piezoelectric materials contain micron-sized regions, generally referred to as the Weiss domains, which possess a permanent dipole moment. The orientation of such dipole moments in different Weiss domains in a virgin (un-poled) piezoelectric material is random and, hence, there is no net dipole moment at the macroscopic length scale. One of the most common ways in which piezoelectric materials are utilized in mechanical actuation applications is through the use of so-called ‘piezoelectric bimorph actuators’. A schematic of a piezoelectric bimorph actuator is shown in Figure (C-1) [49].

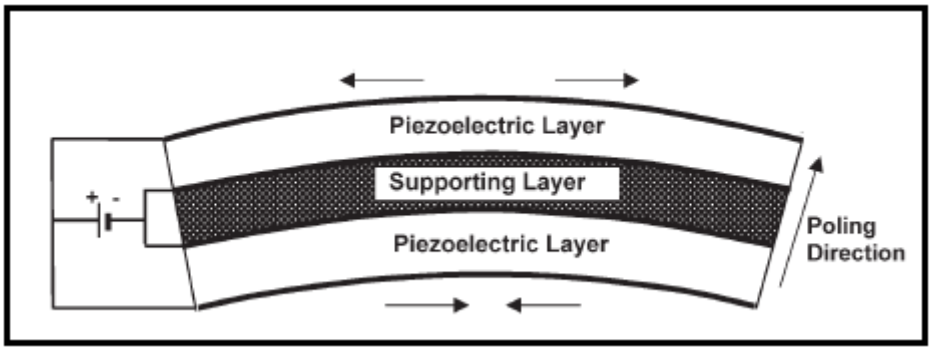

Figure (C-1) A Schematic Of A Piezoelectric Bimorph Actuator. Heavy Lines On Top And Bottom Of Each Layer Are Used To Denote Conductive Metallic Electrodes [49].

When two bimorph actuators are combined and driven by opposite electric fields, they can be used to create a simple grasping/holding device. A schematic of such a grasping device in its open and its fully-closed positions is shown in Figures (C-2) (i) and (ii), respectively.

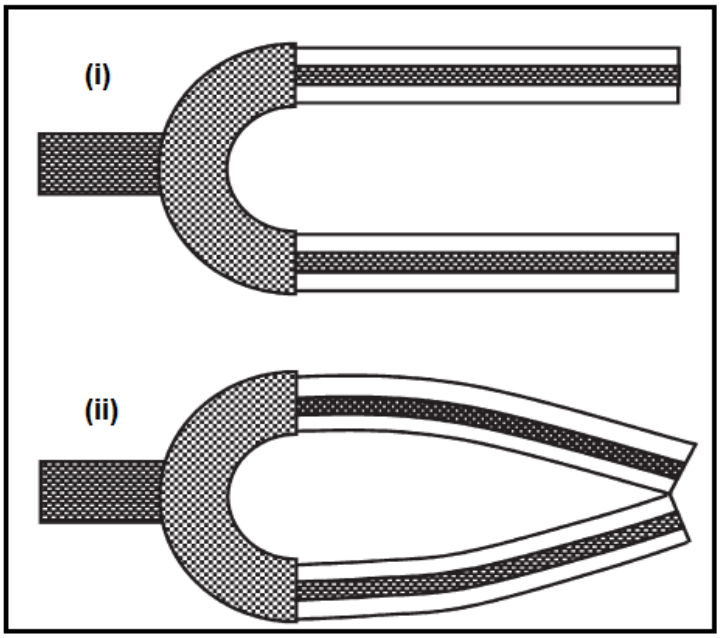

Figure (C-2) A Schematic Of A Piezoelectric Bimorph Grasper In The (i) Open And (ii) Fully-Closed Positions [49].

Appendix (A)

A-1 Accessories and Tools of Laparoscopic Surgery

(1) Veress Needle: The Veress needle is designed to create pneumoperritoneum prior to insertion of trocar in a closed fashion Figure (A-1). It consists of an outer sharp cutting needle and inner blunt spring-loaded obturator.

Figure (A-1) Veress Needle

(2) Open Access Trocars: Hasson's cannula: The Hasson's cannula Figure (A-2) is used for gaining initialaccess to the abdominal cavity with an open cut down technique. It hasa conical blunt tip that is fitted into the cut down site and buttressed in place with fascial sutures attached to the wings of the cannula.

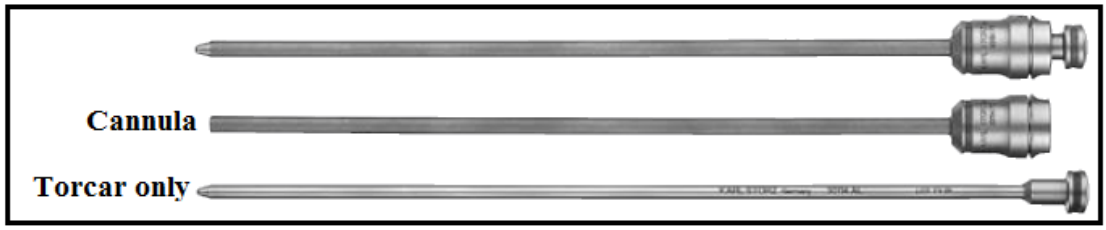

(i)

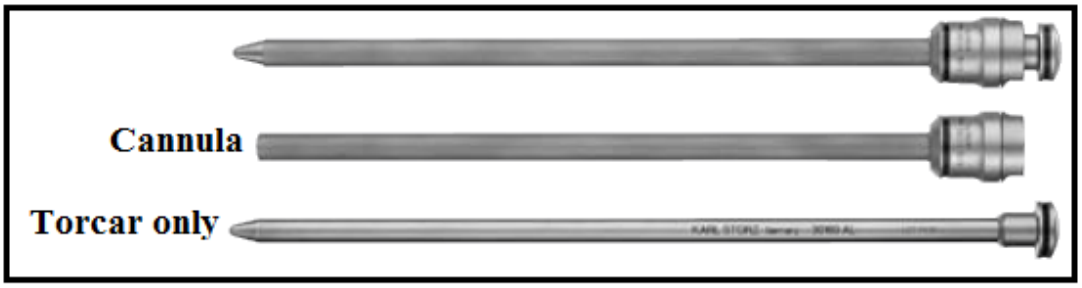

(ii)

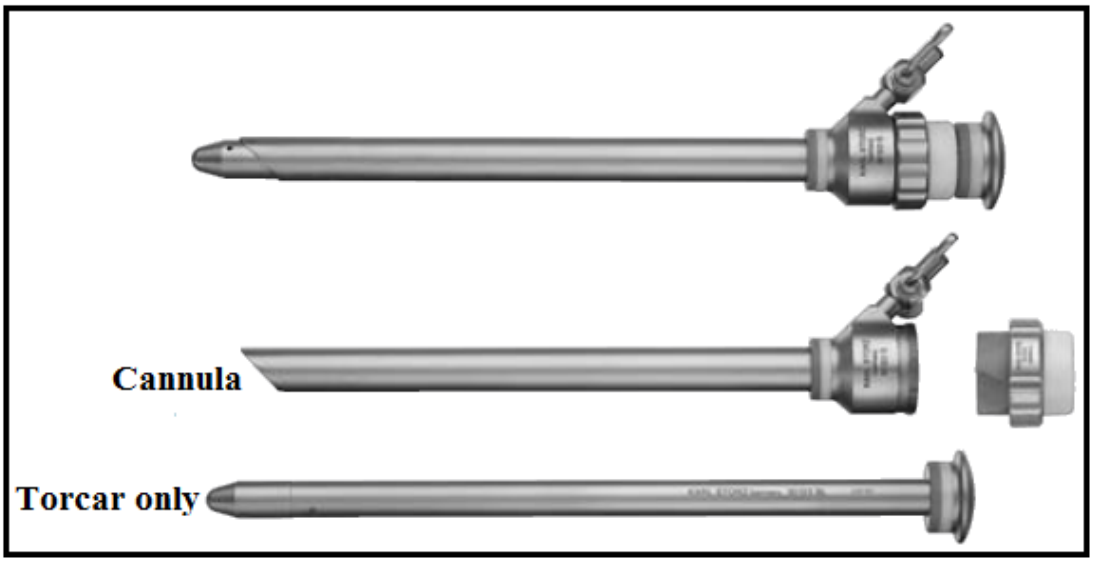

(iii)

Figure (A-2) Open Access Trocars

(i)-CURCILLO-KING Trocars, size 3.5 mm without connector for insufflations with sealing cap, with valve, for use with instruments size 3 mm, Size: 3.5 mm and Working length15 cm.

(ii)- CURCILLO-KING Trocars, size 6 mm without connector for insufflations with sealing cap, with valve, for use with instruments size 5 mm Size: 6 mm and Working length15 cm.

(iii)- Trocars, size 11 mm with connector for insufflation (angled 45°) for use with instruments size 10 mm Size: 11 mm and Working length 15 cm.

(3) <u>Optical Trocar</u>: Optical trocar Figure (A-3) allows visualization of the tissues as the blade cuts through the layers of the abdominal wall.

Figure (A-3) Optical trocar

(4) Gasless laparoscopy: Figure (A-4) as shown, this has some theoretical advantages in some high-risk patients with compromised cardio-respiratory function, decreased diaphragmatic splinting. It facilitates continuous suction and use of some conventional open instruments. However, the exposure may be sub-optimal due to tent like retraction of the abdominal wall. There may be localized trauma to the abdominal wall, parietal peritoneum resulting in more pain.

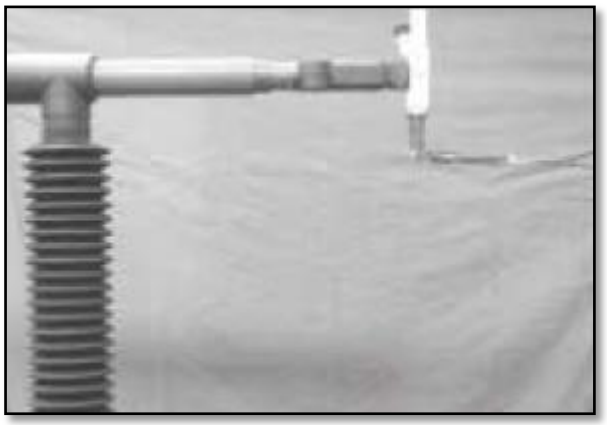

Figure (A-4) Gasless laparoscopy

(5) <u>Light Source</u>: White light illumination is provided from a high-intensity xenon, mercury, or halogen lamp and delivered via a fiber optic bundle Figure (A-5).

Figure (A-5) Light Source

(6)-<u>Light Cable</u>: Light is transmitted from the lamp to the laparoscope through cables. There are two types of cables: fiber optic and fluid. Fiber optic cables are flexible but do not transmit a precise light spectrum. Fluid cables transmit more light and a complete spectrum but are more rigid. Fluid cables require soaking for sterilization and cannot be gas sterilized, see Figure (A-6).

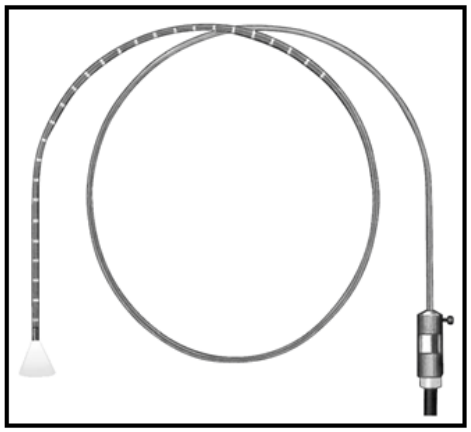

Figure (A-6) Light Cable

ABSTRACT

This thesis presents a study for optimal design of a robot to be used in human surgery (Laparoscope device). It was done in Al-Sader educational hospital in Maysan Governorate. The robot was manufactured by Karl Storz company. Connecting linkages were increased to get seven degrees of freedom. It is operated by the surgeon hand (complete rotation 360^{o} , rotation in two opposite directions perpendicular to each other ,transformation along the major axes , triple joint (pitch ,roll, and yaw) . Optimization has been done to these models after making analysis to the surgical robot (forward kinematic, inverse kinematic, dynamitic analysis).

The optimal design was obtained by using genetic algorithm method to choose the optimal path planning in the working area. This was with the presence of obstacles to tip of end-effector motion that exists, in mechanical arm to the new model that used in this thesis. This was done by making an integrated computer program through MATLAB (R2013a). The results of best path planning would shorten length without hitting any obstacle, assuming the surrounding environment will be variable. The position and obstacle shapes would be random. We found that the best path planning in every environment depends on maximize objective function that presented by shortest length of the path. This is important from the medical point of view. This was applied successfully in practice on an industrial robot and the resulted optimal parameters to that robot with matching of the theoretical side with practical side in robot motion. The practical side was made in laboratory of the Research Unit of Automation and Robotics in the

Control and Systems Engineering Department, University of Technology. The robot used was the Lab-Volt Servo Robot System Model 5250 (RoboCIM5250).

This thesis includes studying the tools used in laparoscope and focuses on recent types of graspers with parallel jaws connected to the chosen design. It was noticed that the maximum entrance force for the abdominal tracar must not exceed 5N. The force on the last point of jaws is 0.42N. It was found that this force will not cause bleeding in the tissue during procedure. And that this type of small size grasper can be bent during operation in the allowed field of workspace while maintaining good strength.

CONTENTS

LIST OF FIGURES

LIST OF TABLES

LIST OF SYMBOLS

Symbol	Meaning	Unit
$\mathbf{a}_i$	The link i length	mm
$c\boldsymbol{\theta}_i$	Cos function of $\boldsymbol{\theta}_i$ joint angle	-
$c\boldsymbol{\alpha}_{i-1}$	Cos function of $\boldsymbol{\alpha}_{i-1}$ twist angle	-
$\mathbf{d}_4$	The length of translation joint of model	mm
$\mathbf{d}_i$	The link offset	mm
$\dot{d}_{i+1}$	The velocity of prismatic joint of model	mm/sec
$\boldsymbol{f}_i$	Force exerted on link i by link i - 1,	N
${}^{i}\boldsymbol{f}_{i+1}$	Force exerted on link (i+1) by link i	N
$\mathbf{i}$	The number of joint	-
$\mathbf{JF}_1,\mathbf{JF}_2,$ $\mathbf{JF}_3,\mathbf{JF}_4$	Applied Forces on Parallel Jaws	N
$\boldsymbol{J(\theta)}$	Jacobian matrix	-
$\mathbf{L}_1$	The length of first link of model	mm
$\mathbf{L}_3$	The length of third link of model	mm
, $\mathbf{n}_i$	torque exerted on link i by link i - 1.	N.m
${}^{i}\boldsymbol{n}_{i+1}$	Torque exerted on link i+1 by link i	N.m
$\mathbf{p}_x$	The position of end-effector at x-axis	mm
$\mathbf{p}_y$	The position of end-effector at y-axis	mm
$\mathbf{p}_z$	The position of end-effector at z-axis	mm
${}^{i}\mathbf{P}_{i+1}$	Vector offset between origins between frame {i} to frame {i+1}.	-
${}^{i}_{i+1}\boldsymbol{R}$	Rotation matrix from i+1 to the i joints	-
$s\boldsymbol{\theta}_i$	Sin function of $\boldsymbol{\theta}_i$ joint angle	-
$s\boldsymbol{\alpha}_{i-1}$	Sin function of $\boldsymbol{\alpha}_{i-1}$ twist angle	-
${}^{i-1}_{i}\boldsymbol{T}$	Transformation matrix from i to the i-1 joints	-
${}^{base}_{end-effector}\boldsymbol{T}$	Transformation matrix from the last joint to the base joint	-
${}^{i}\vec{\boldsymbol{v}}_i$	Linear velocity of the origin of frame {i} relative to the reference frame {O} (fixed), expressed in {i}	m/sec.

$^{i}\vec{v}_{i+1}$	The linear velocity frame {i+1} is moving relative to frame {i}	m/sec.
$\dot{x}$	The velocity of end-effector at x-axis	mm/sec.
$\dot{y}$	The velocity of end-effector at y-axis	mm/sec.
$\dot{z}$	The velocity of end-effector at z-axis	mm/sec.

LIST OF GREEK LETTERS

Symbol	Description	Units
α_{i-1}	The twist angle of the link	degree
θ_i	The joint angle	degree
$\dot{\theta}_{i+1}$	The joint velocity of link i+1	rad/sec.
Δb	The backward horizontal motion of grasper jaws during opening	mm
Δx	The horizontal shaft motion	mm
Δz	The jaw opening width	mm
$^{i}\omega_i$	Angular velocity of frame {i} relative to the reference frame {O} (fixed), expressed in {i}	rad/sec.
$^{i+1}\vec{\omega}_{i+1}$	The angular velocity of link i + 1 with respect to frame {i + 1}	rad/sec.
ω_x	The angular velocity of end-effector at x-axis	rad/sec.
ω_y	The angular velocity of end-effector at y-axis	rad/sec.
ω_z	The angular velocity of end-effector at z-axis	rad/sec.
$^{i}\Omega_{i+1}$	Rotational velocity of frame {i+1} relative to frame {i}.	rad/sec.
τ	linear joint force	N

ABBREVIATIONS

Abbreviation	Meaning
ADM	Aggregated Dexterity Measure
CCD	Charge-Coupled Device
CT	Company Tax guidance
CO_2	Carbon Dioxide
DLR	multi-arm surgical system (medical robot)
D-H	Denavit- Hartemberg parameters
DOF	Degree Of Freedom
EA	Evolutionary Algorithm
EDWS	Electron Discharge waves
FL	Fuzzy Logic
FLM	Fuzzy Logic Methodology
FWM	Friction Wheel Mechanism
GA	Genetic Algorithm
H.T	Homogenous matrix
IAE	Integral of Average Error
ISE	Integral Squared Error
ITAE	Integral Time-weighted Absolute Error
ITSE	Integral of Time multiplied by the Squared Error
LSTM	Long Short-Term Memory
MATLAB	Matrix Laboratory
MEMS	Micro Electro -Mechanical Systems
MIS	Minimally Invasive Surgery
OR	Operating Room
PARASURG 5M	Parallel Surgical Robot with five degree of freedom
PID	Proportional-Integral-Derivative
PUMA	Programmable Universal Machine for Assembly, or Programmable Universal Manipulation Arm
RCM	Remote Center of Motion
RMIS	Robot-assisted Minimally Invasive Surgery
RMS	Root Mean Square
RNNs	Recurrent Neural Networks

REFERENCES

[1]. Kuo Chin-Hsing , Dai Jian S. and Dasgupta Prokar,” Kinematic Design Considerations for Minimally Invasive Surgical Robots: An Overview”, The International Journal of Medical Robotics and Computer Assisted Surgery, Vol. 8, Issue 2, pp. 127-145, 2012. http://www.ivsl.org.

[2]. Frank Tendick, S. Shankar Sastry, Ronald S. Fearing, and Michael Cohn, "Applications of Micromechatronics in Minimally Invasive Surgery", IEEE Transactions on Mechatronics, Vol. 3, No. 1, March 1998.

[3]. Nabil Simann,” Analysis and Synthesis of Parallel Robots For Medical Applications “, Msc. in Mechanical Engineering, The Institute of Technology, ISI, Haifa,1999.

[4]. Jocelyne Troccaz, Michael Peshkin and Brian Davies, "The Use of Localizers, Robots and Synergistic Devices in CAS**",** J. Computer Science Vol. 1205, pp 725-736**,**1997.

[5]. Wen P. Liu, Jonathan M. Sorger and Russell H. Taylor,” Toward Intraoperative Image-Guided Transoral Robotic Surgery”, Journal Robotic Surg, © Springer-Verlag London 2013.

[6]. Russell H. Taylor and Dan Stoianovici, "Medical Robotics and Computer-Integrated Surgery", IEEE Transactions on Robotics and Automation, Vol. 19, No. 5, October 2003.

[7]. Patrick A. Finlay, "Surgical Robotics State of the Art and Future Trends", Prosurgics Ltd, High Wycombe UK, March 2007.

[8]. Murat Cenk, Michael Cohnb, Frank Tendickc and Shankar Sastrya, "Laparoscopic Telesurgical Workstation", IEEE Transactions on Robotics And Automation, Vol. 15, No. 4, August 1999.

[9]. Linda van den Bedem, "Realization of a Demonstrator Slave for Robotic Minimally Invasive Surgery", Ph.D. thesis, University Eindhoven, Netherlands, 22 September 2010.

[10]. Davide Lomanto, "Manual of Laparoscopic Surgery", Ph.D., National University Hospital Singapore, 2004.

[11]. Prajapati P M., Solanki A S. and Sen D J.," Robotics Surgery: A New Hope IN Medical Science", International Research Journal Of Pharmacy, Vol.3, No.1,2012

[12]. Karthiga Mohan, "An Improved Path Planning REB Mechanism For Rescue Robot In Unmanned Areamore", International Journal of Scientific Engineering and Research , Vol.2, Issue3, 2014.

[13]. Ismail AL-Taharwa, Alaa Sheta and Mohammed Al-Weshah, " A Mobile Robot Path Planning Using Genetic Algorithm in Static Environment", Journal of Computer Science, Vol. 4,No. 4, pp. 341-344, 2008.

[14]. Tamilselvi, Mercy shalinie and Hariharasudan, " Optimal Path Selection for Mobile Robot Navigation Using Genetic Algorithm", International Journal of Computer Science Issues, Vol. 8, Issue 4, No. 1, 2011.

[15]. Daniel Porto, "Design Methodology and Numerical Optimization of Ultrasonic Transducers for Spinal Surgery", Ph.D. thesis, Lausanne, 2009.

[16]. Takashi Suzuki, Yoichi Katayama, Etsuko Kobayashi and Ichiro Sakuma, "Mechanical error analysis of compact forceps manipulator for laparoscopic surgery", I-Tech Education and Publishing, Vienna, Austria, 2005.

[17]. Pablo Lamata de la Orden, "Methodologies for the Analysis, Design and Evaluation of Laparoscopic Surgical Simulators", UCL Presses Universities De Louvain, 2004.

[18]. Papanikolaidi I., Synodinos A., Moulianitis V.C., Aspragathos N. and Xidias E.K., "Optimal Base Blacement of the Da Vinci System Based on the Manipulability Index", Proceedings of the RAAD 22nd International Workshop on Robotics in Alpe-Adria-Danube Region, Slovenia, September 11-13, 2013.

[19]. Yun-Ju Lee, Jonathan Kim, Seong-Young Ko, Woo-Jung Lee and Dong-Soo Kwon, " Design of a Compact Laparoscopic Assistant Robot KaLAR", International Conference on Control, Automation, and Systems (Gyeongju, Korea),2003.

[20]. Shyam Venugopal, Lun-Chen Hsu, Smitha Malalur, Wang B.P., Mu Chiao and Chiao J.-C., "Design and Modeling of a High Accuracy, Three Degree of Freedom MEMS Manipulator", Proc. SPIE 6037, Device and Process Technologies for Microelectronics, MEMS, and Photonics, Australia, 2005.

[21]. Christopher R. Wagner and Robert D. Howe, "Force Feedback and Visual-spatial Ability in Multi Degree of Freedom Robotic Surgery", IEEE, Division Of Engineering and Applied Sciences, Harvard University, Cambridge, Vol.23 , No.6, pp. 1235 - 1240, 2007.

[22]. Pisla D., Gherman B., Plitea N., Gyurka B., Vaida C., Vlad L., Graur F., Radu C., Suciu M., Szilaghi A. and Stoica A., "PARASURG Hybrid Parallel Robot For Minimally Invasive Surgery", Chirurgia (Romania), Copyright© Celsius, Vol. 106, pp. 619-625, 2011.

[23]. Taoming Liu, "Design and Prototyping of a Three Degrees of Freedom Robotic Wrist Mechanism for a Robotic Surgery

System", Thesis of Master of Science, Department of Mechanical and Aerospace Engineering, Spain, 2011.

[24]. Duck Hee Lee, SeungJoon Song, Reza Fazel-Rezai and Jaesoon Choi, "The preliminary results of a force feedback control for Sensorized Medical Robotics", International Journal of Advanced Research in Artificial Intelligence, Volume 2, No.5, 2013.

[25]. http://ieeexplore.ieee.org , Veronica Garcıa-Perez, Emma Munoz-Moreno, Rodrigo de Luis-Garcıa and Carlos Alberola-Lopez, " A 3D Collision Handling Algorithm for Surgery Simulation Based on Feedback Fuzzy Logic", Information Technology in Biomedicine, IEEE Transactions , Vol.13, No. 4, 2009.

[26]. Farzin Piltan, Ali Badri, Javad Meigolinedjad and Mohammad Keshavarz, "Adaptive Artificial Intelligence Based Model Base Controller: Applied to Surgical Endoscopy Telemanipulator", International Journal of Intelligent Systems and Applications, Vol. 5, No. 9, August 2013. http://www.ivsl.org

[27]. Seung Joon Song, Youngjin Moon, Duck Hee Lee, Chi Bum Ahn, Youngho Jo and Jaesoon Choi, " A Comparative Study of Fuzzy PID Control Algorithms for Enhanced Position Control in a Laparoscopic Surgery Robot", Journal Med. Biol. Eng., Nov 26, 2013. http://www.ivsl.org

[28]. Hermann Mayer, Faustino Gomez, Daan Wierstra, Istvan Nagy, Alois Knoll, and Jurgen Schmidhuber, " A System for Robotic Heart Surgery that Learns to Tie Knots Using Recurrent Neural Networks", Advanced Robotics , Vol. 22, Issue 13-14, 2008. http://www.ivsl.org

[29]. Auranuch Lorsakul,Chanjira Sinthanayothin and Jackrit Suthakorn, " Optical Marker Recognition and Pose Determination Using Neural Networks: Toward Development of A Dental Surgical Navigation System", Computer Assisted Radiology and Surgery 22nd International Congress and Exhibition, Barcelona, Spain, June 25 - 28, 2008.

[30]. Auranuch Lorsakul, Jackrit Suthakorn, Chanjira Sinthanayothin and Wichit Tharanon, "Toward Robot-Assisted Dental Surgery: Path Generation and Navigation System Using Optical Tracking Approach", Proceedings of the IEEE International Conference on Robotics and Biomimetics Bangkok, Thailand, February 22 - 25, 2009. http://libhub.sempertool.dk.tiger.sempertool.dk.

[31]. Sergiu-Dan Stan, Vistrian Maties and Radu Balan, " Optimization of a 2 DOF Micro Parallel Robot Using Genetic Algorithms", 4th IEEE International Conference, Kumamoto , 8-10 May 2007. http://ieeexplore.ieee.org.tiger.sempertool.dk .

[32]. Papanikolaidia A., Synodinos V.C., Moulianitis, N. and Aspragathos E.K. ," Optimal Base placement of the Da Vinci System based on the Manipulability Index", 22nd International Workshop on Robotics, Slovenia, September 11-13, 2013.

[33]. Rainer Konietschke, Tobias Ortmaier, Holger Weiss, Robert Engelke, and Gerd Hirzinger, "Optimal Design of a Medical Robot for Minimally Invasive Surgery", Munich University of Technology, Institute of Applied Mechanics, November 2003. http://www.robotic.dlr.de .

[34]. Gonchar L. E., Engel D., Raczkowsky J., and Wörn H., "Simulation for Path Planning and Motion Control for Medical Robot", The Workshop on Computer Science and Information Technologies, Russia, 2000.

[35]. Louaï Adhami and Ève Coste-Manière, "Optimal Planning for Minimally Invasive Surgical Robots", IEEE Transaction on Robotics and Automation, Vol. 19, No. 5, October 2003.

[36]. Mitchell J.H. Lum, Jacob Rosen, Mika N. Sinanan, Blake and Hannaford, "Kinematic Optimization of a Spherical Mechanism for a Minimally Invasive Surgical Robot", Proceedings of the IEEE International Conference on Robotics & Automation, New Orleans, April 2004. http://ieeexplore.ieee.org .

[37]. Rainer Konietschke, Tobias Ortmaier, Ulrich Hagn, GerdHirzinger, and Silvia Frumento, "Kinematic Design Optimization of an Actuated Carrier for the DLR Multi-Arm Surgical System", International Conference on Intelligent Robots and Systems, Beijing, China October 9 - 15, 2006.

[38]. Xueyi Zhang and Li Zou," Design Optimization of a Minimally Invasive Surgical Robot". IEEE International Conference, Shenzhen , 20-24 March 2007. http://ieeexplore.ieee.org.tiger.sempertool.dk .

[39]. Ruqi Ma , Harbin Inst, Weidong Wang , Zhijiang Du and Gang Li, " Design And Optimization Of Manipulator For Laparoscopic Minimally Invasive Surgical Robotic System**,** IEEE International Conference, Mechatronics and Automation, Chengdu, 2012. http://www.ivsl.org

[40]. Wael A. Al-Tabey, "Effect of Trajectory Planning Duration Time On Correct Dynamic Response Selection Of Micro-Robot For Surgical Application", African Journal of Engineering Research Vol. 1(3), pp. 75-83, July 2013.

[41]. Ali Hassan Zahraee, Jamie Kyujin Paik, Jrome Szewcyzk, and Guillaume Morel, " Towards the Development of a Hand-Held Surgical Robot for Laparoscopy", Mechatronics, IEEE/ ASME Transactions IEEE,Volume:15 , Issue: 6 , Pages: 853 – 861, 2010.

[42]. KARL STORZ ,Endoscope – Catalog. https://www.karlstorz.com.

[43]. A. Melzer, G. Buess, and A. Cuschieri, "Instruments for Endoscopic Surgery," Operative Manual Of Endoscopic Surgery – Springer Verlag, pp. 15, 1989. https://www.karlstorz.com.

[44]. KARL STORZ GmbH & Co. KG., "Laparoscopy In Surgery, Gynecology, Urology", 7th Edition, 2012. http://www.linkster.sk/IMAGES/storz_laparoscopy.pdf.

[45] Lai F. and Howe R., "Evaluating Control Modes For Constrained Robotic Surgery," IEEE International Robotics and Automation Conference, Volume:1, 2000.

[46]. John J. Craig," Introduction to Robotics Mechanics and Control", Pearson Prentice Hall, Third Edition,2005. http://ieeexplore.ieee.org.

[47]. Berkelman, P.J., Albert Bonniot, Tronche La, Whitcomb, L.L. ; Taylor, R.H. and Jensen P.," A miniature microsurgical instrument tip force sensor for enhanced force feedback during robot-assisted manipulation", Robotics and Automation, IEEE Transactions , Vol. 19 , Issue: 5 ,2003

[48].John Vlot," Optimizing Working Space in Laparoscopy", PhD thesis, Medical School at Erasmus, University Rotterdam,2014.

[49]. Grujicic M., Zhao C. L., and Austin E. M.," Optimization of a piezoelectric bimorph grasper for use in minimally invasive surgical applications", Journal Engineering Manufacture, Vol. 219, Part B, 2005.

[50]. Veronika Ivanova, Krassimira Koleva, Radko Mihailov and Iossif Beniozef," Family Tools For Robot-Assisted Surgery", Manufacturing Systems, Volume 8, Issue 2, 2013.

[51]. Schier F. and Turial S.," Technical Basics: Insufflation, Trocar Insertion, Instruments, Needle Insertion, Suturing, Ligating", (C) Springer-Verlag Berlin Heidelberg, 2013. http://media.axon.es.

[52]. Khashayar Vakili , Mattias Flander, Toomas Sepp, Juan Diaz and Alexander Slocum," Design And Testing of A Pressure Sensing Laparoscopic Grasper", The Design of Medical Devices Conference Minneapolis, Mn, USA, April 12-14 ,2011. http://stuff.mit.edu.

[53]. Sara Bergstrand," Tissue Blood Flow Responses to External Pressure using LDF and PPG", Printed in Swedan By LiU-Tryck, Linkoping, Swedan,2009.

[54]. Alexandre Krupa, Guillaume Morel and Michel De Mathelin," Achieving High-Precision Laparoscopic Manipulation Through Adaptive Force Control", Journal Advanced Robotics, Vol. 18, No. 9, pp. 905–926 ,20l04.

[55]. Amel Serrat and Mohamed Benyettou, "GA-SVM and MLP-BBO to estimate Robot Manipulator Joint Angles", International Journal of Soft Computing and Engineering (IJSCE), Vol, 3, Issue-5, November 2013.

[56]. Ngah J. Wan and Mohamad Z.,"Point to Point Sensor Based Path Planning Algorithm for Mobile Robots", International Conference on System Science and Simulation in Engineering (ICOSSSE) , Iwate, Japan, 2010. http://www.wseas.us.

[57]. Zhou Chang ,"Fundamentals of Genetic Algorithms", The 2nd International Conference on Computer Application and System Modeling, 2012. http://www.ivsl.org

[58]. Hagen Burchardt and Ralf Salomon, " Implementation of Path Planning using Genetic Algorithms on Mobile Robots", In IEEE

World Congress on Computational Intelligence (WCCI), pp. 1831-1836, July 2006.

[59]. Tamil Selvi, Mercy Shalinie and Harihar Asudan," Optimal Path Selection for Mobile Robot Navigation Using Genetic Algorithm", International Journal of Computer Science Issues, Vol. 8, Issue 4, No 1, July 2011.

[60]. Raja P. and Pugazhenthi S., "Optimal path planning of mobile robots: A Review", International Journal of Physical Sciences, Vol.7, No. 9, pp. 1314 - 1320, 2012.

[61]. Saska M., Macas M., , Preucil L. and Lhotska L., "Robot Path Planning using Particle Swarm Optimization of Ferguson Splines", IEEE International Conference on Emerging Technologies and Factory Automation , Prague, Czech Republic, 20-22 Sept., 2006.

[62]. Wahab Aminiazar, Farid Najafi and Mohammad Ali Nekoui, "Optimized Intelligent Control of a 2 Degree of Freedom Robot for Rehabilitation of Lower Limbs using Neural Network and Genetic Algorithm", Journal of Neuro Engineering and Rehabilitation, 2013. http://www.jneuroengrehab.com .

[63]. Nadia Adnan Shiltagh and Lana Dalawr Jalal," Path Planning of Intelligent Mobile Robot Using Modified Genetic Algorithm", International Journal of Soft Computing and Engineering, Vol. 3, Issue-2, May 2013.

[64]. Ismail AL-Taharwa, Alaa Sheta and Mohammed Al-Weshah, " A Mobile Robot Path Planning Using Genetic Algorithm in Static Environment", Journal of Computer Science, Vol. 4,No. 4, pp 341-344, 2008

[65]. Chuanling Liu , Huaiwang Liu and Jingy Yang," A Path Planning Method Based on Adaptive Genetic Algorithm for Mobile Robot",

Journal of Information & Computational Science, Vol. 8: No. 5, pp. 808–814, 2011.

[66]. Michael N.Helmus, "Biomaterials in the Design and Reliability of Medical Devices", Print in USA, ISBN:1-58706-039-6, 2002. http://www.landesbioscience.com

الخلاصـــــــــــــــة

تناولت هذه الرسالة دراسة تصميم امثل لموديل مختار للإنسان الآلي المستخدم في مجال الجراحة البشرية (جهاز التنظير البطني الجراحي) المستخدم في مستشفى الصدر التعليمي في محافظة ميسان و المصنع من قبل شركة (KARL STORZ) من خلال زيادة عدد درجات الحرية لتصل سبعة درجات الحرية تم ذلك بزيادة وصلات الاتصال وهي كما يلي ابتدءا من الماسكة الرئيسية ليد الجراح (دوران كامل ٣٦٠° ، دوران ١٨٠° باتجاهين متعاكسين متعامدين على بعضهما , حركة الانتقالية على طول المحور الرئيسي، مفصل ثلاثي ويشمل (Roll, Yaw, Pitch) وتم أجراء التحليل لموديل الجديد وكما يلي:

(Forward Kinematic, Inverse Kinematic And Dynamic Analysis).

تم اعتماد تصميم الأمثل وذلك باستخدام طريقة الخوارزمية الجينية لأختار المسار الأمثل في مجال العمل المحدد وبوجود العوائق أمام حركة Tip of End-effector الموجودة في الذراع الميكانيكي للموديل الجديد الذي استخدم في هذه الرسالة وتم ذلك بإنشاء برنامج حاسوبي متكامل عن طريق لغة (MATLAB R2013a) وكان الحصول على أفضل مسار والذي يكون الأقصر طولا وبدون الاصطدام بأي عائق وتم الافتراض أن البيئة المحيطة تكون متغيرة وكذلك مواقع و أشكال العوائق بحيث تكون عشوائية، فقد تم الحصول على أفضل مسار في كل بيئة بالاعتماد على (Objective Function) لأهمية ذلك في المجال الطبي. و بالاعتماد على الجانب النظري الذي تم الحصول على نتائج جيدة طبق ذلك عمليا بنجاح على روبوت صناعي والحصول على (Optimal Parameters) لذلك الروبوت مع تطابق الجانب النظري والعملي بحركة الروبوت على المسار الأمثل الذي تم اختياره. وتم اجراء الجانب العملي في مختبر وحدة الانسان الآلي والاتمتة في قسم هندسة السيطرة والنظم / الجامعة التكنولوجية وكان الروبوت المستخدم هو

The Lab-Volt Servo Robot System Model 5250(RoboCIM5250)

تضمنت هذه الرسالة دراسة الأدوات التي تستخدم في جهاز التنظير البطني الجراحي وتم التركيز على احدث نوع من القابضات ذات الماسكات المتوازية التي تم ربطها مع الموديل المختار مع ملاحظة أن أقصى قوة دخول الحاجز البطني يجب لا تتجاوز 5N. أما مقدار القوة

عند أخر نقطة في الماسكات هي 0.42 N وجد أن مقدار هذه القوة لا تسبب نزيف في الأنسجة أثناء العمل. وجد أن هذا النوع من القابضات صغيرة الحجم ويمكن أن تنحني أثناء العمل في مجال المسموح العمل فيه وكذلك ذات متانة جيدة.

Ministry of Higher Education and Scientific Research University of Technology Electromechanical Engineering Department

Path Optimization for Medical Surgery Robotic Using Genetic Algorithm

A Thesis

Submitted to the Department of Electromechanical Engineering of the University of Technology in a Partial Fulfillment of the Requirements for the Degree of Master of Science in Electromechanical Engineering/ Electromechanical Systems Engineering

By

Zahraa Dawood Hussein

Supervised by

Asst. Prof. Dr. Muhannad Z. Khalifa **Dr. Iman S. Kareem**

2014 **1435**

وزارة التعليم العالي و البحث لعلمي
الجامعة التكنولوجية
قسم الهندسة الكهروميكانيكية

المسار الامثل للجراحة الروبوتية الطبية باستخدام الخوارزمية الجينية

رسالة

مقدمة إلى قسم الهندسة الكهروميكانيكية في الجامعة التكنولوجية وهي جزء
من متطلبات نيل درجة الماجستير في علوم
الهندسة الكهروميكانيكية / هندسة النظم الكهروميكانيكية

مِن قِبَل

زهراء داود حسين

بإشراف

أ.م.د. مهند زيدان خليفة

م.د. إيمان صالح كريم

٢٠١٤م

١٤٣٥هـ